NYO-2262-121

ANALYTICITY PROPERTIES OF THE MESON-DEUTERON ELASTIC-SCATTERING AMPLITUDES AT LOW ENERGY*

Fujio Ando** and David Feldman

Department of Physics

Brown University

Providence, Rhode Island

Submitted to the Supplement
of Progress of Theoretical Physics
in honor of Professor S. Tomonaga

---

*This work was supported, in part, by the U. S. Atomic Energy Commission (Report No. NYO-2262-121).

**On leave of absence from the Virginia Polytechnic Institute, Blacksburg, Virginia during the 1965-66 academic year.

Analyticity Properties of the Meson-Deuteron Elastic-Scattering Amplitudes at Low Energy*

Fujio Ando** and David Feldman
Department of Physics
Brown University
Providence, Rhode Island

ABSTRACT

A dispersion-theoretic treatment of the elastic scattering at low energy of mesons by deuterons is presented. The loosely bound nature of the deuteron results in small anomalous thresholds of the scattering amplitudes in the t channel and justifies the use of selected Feynman diagrams in the determination of the general analyticity properties of the amplitudes. The impulse approximation, binding corrections, and multiple-scattering terms are defined in terms of both triangle and box diagrams, and the dispersion relations with fixed s for these terms are derived by the method of analytic continuation with respect to the deuteron mass and with respect to s. It is found that the anomalous parts of the deuteron-baryon vertices play important roles in the derivation of the dispersion relations, and that the double-scattering amplitudes have no complex singularities.

The general method has been applied to a determination of the angular distributions for $\pi^{\pm}d$ and $K^{-}d$ elastic scattering. In the former case, the binding corrections due to $N^{*}_{3/2}$ is the main correction to the impulse approximation. In the latter case, the impulse approximation has been determined in terms of the $\bar{K}N$ scattering amplitudes which are approximated by two complex poles.

---

*This work was supported, in part, by the U. S. Atomic Energy Commission (Report No. NYO-2262-121).

**On leave of absence from the Virginia Polytechnic Institute, Blacksburg, Virginia during the 1965-66 academic year.

I. INTRODUCTION

The deuteron is a bound state of a proton and a neutron and has apparently the simplest structure of any stable composite particle. Although its static and dynamic properties would appear at first sight to be easily derivable from a consideration of the two-body nucleon-nucleon system, a consistent field-theoretic treatment is not yet available.[1-3] Despite this, it is eminently desirable to consider the development of methods for handling even more complicated systems, consisting of three bodies, say (two nucleons plus a meson), which may even cast some light on the properties of the two-nucleon system. In this paper, we shall be concerned with the study of reaction processes involving the deuteron, and, in particular, with pion-deuteron (πd) and kaon-deuteron ($\bar{K}d$) elastic scattering.

It is well known[4] that the binding energy of the deuteron is very small (2.226 MeV) compared to the average binding energy of a nucleon in a nucleus (6-7 MeV). This property of the deuteron manifests its loosely bound character. This results in the following important assumption in the study of the collision of a particle (a nucleon or pion, for example) with a deuteron. If the incident particle has a kinetic energy of about 100 MeV, then the binding energy of the deuteron is negligible and the deuteron can be regarded as made up of two free nucleons during the collision. The nucleon-deuteron (Nd) or πd scattering amplitudes can then be expressed in terms of the two-body NN or πN scattering parameters. This procedure corresponds to the impulse approximation[5-7] (IA) and has been applied successfully[8,9] to various high-energy scattering problems. It is evident that, as the kinetic energy of the incident particle decreases, corrections to the IA due to the nuclear force binding the deuteron become important.

We proceed at this point to summarize briefly the current experimental as well as theoretical situations for the cases of πd and $\bar{K}d$ scattering.

Since 1952, many attempts[10-14] have been made to carry out measurements of πd scattering, with the first complete and accurate results being obtained by Rogers and Lederman[15] in 1957. They determined the angular distribuions for the elastic and inelastic scattering of a π^+ meson by a deuteron target at 85 MeV (laboratory energy) as well as the corresponding total cross sections. Insofar as the elastic scattering is concerned, the angular distribution is generally dominant at small angles but drops sharply as the scattering angle tends to zero. This sharp depression in the extreme forward direction is due to interference between the Coulomb and strong interactions. If Coulomb effects are subtracted out, the angular distribution has a fairly simple structure with a dominant forward peak. There is a minimum at about 80° (laboratory angle) with a slight increase in the backward direction.

The impulse approximation was first applied to πd scattering by Fernbach, Green, and Watson,[8] with the first detailed treatment being carried out by Rockmore.[16] In either case, the IA was interpreted to mean that the overall scattering amplitude can be expressed as a linear superposition of πN scattering amplitudes, where the latter are, in turn, given in terms of the experimentally determined πN phase shifts. This definition of the IA involves neglecting not only the nuclear force binding the deuteron during the scattering, but also multiple scattering; it also ignores the fact that the πN matrix elements that arise in πd scattering are off the energy shell. The angular distribution resulting from Rockmore's calculations, which are based on these approximations but do take Coulomb effects into account, agrees very well with the Rogers and Lederman measurement at 85 MeV.

Rockmore also estimated multiple-scattering and binding corrections to the total cross section for πd scattering (elastic plus inelastic) as calculated within the IA. In particular, the effect of double scattering as well as higher-order multiple scattering, when calculated in terms of Brueckner's t-matrix formalism,[17] is to enhance the total cross section. Within the limitations of this calculation, the double scattering appears to be the most important of the multiple-scattering corrections.[17,18] Rockmore, by calculating the double scattering in perturbation theory, has suggested, however, that the Brueckner model, which neglects multiple scattering off the energy shell, is not reliable [17,19] at the energies under consideration. The correction due to binding (the potential correction) was estimated[16] in perturbation theory; it leads to a decrease in the total cross section which is of the same order of magnitude as the correction due to multiple scattering. The resultant total cross section in the impulse approximation is then about 10% smaller than the experimental value; Rockmore suggested that an improved value could be obtained by including an absorption term, but evidently this is simply a phenomenological device.

Perhaps the most serious fault of the preceding calculation arises from the fact that one does not know how to extrapolate the πN scattering amplitude to its values off the energy shell. There have been several suggestions[16-19] as to how to treat this problem, but the results are strongly model-dependent. In this sense, therefore, the apparent success of Rockmore's calculation may be entirely fortuitous. We should also mention at this point several attempts[20-22] which have been made at a unified treatment of the impulse approximation, taking the binding and multiple-scattering corrections into account, but still within the framework of a phenomenological theory. However, it should be noted that the off-the-energy-shell amplitude cannot be determined unambiguously within such theories.

We may summarize our discussion of the πd problem to this point by noting that a satisfactory treatment requires the consideration of off-the-energy-shell as well as multiple-scattering and binding corrections to the IA. One way to proceed is to abandon the traditional approach to the impulse approximation and to consider instead a theory of πd scattering based on analyticity and unitarity. In this case there is no ambiguity in the determination of off-the-energy-shell πN matrix elements; also, the IA, as well as the various corrections to it, can be handled within this framework. Such an approach constitutes the fundamental goal of this paper.

We next turn our attention to the K^-d scattering problem. First we note that, unlike the case of πd, K^-d and K^+d scattering are not related by charge symmetry, and the two cases have to be studied separately. In this paper, we will limit our considerations to the more complicated K^-d scattering problem, the simpler K^+d scattering being readily understood in terms of standard impulse-approximation techniques.[23]

Not many K^-d scattering experiments have been performed at low energy (below 100 MeV). The only data available at present are those of the Alvarez group[24] on the sum of the elastic K^-d as well as inelastic ($K^-d \to K^-pn$) scattering for 15.5, 29.6, and 42.3 MeV (laboratory energy) K^- particles. The differential cross section has not been measured so far, nor has the elastic scattering been as yet separated from the inelastic (although Horwitz et al.[25] are attempting to do just this). While the experimental situation is thus still obscure, a number of calculations[26-29] of K^-d scattering have been put forward. In principle, K^-d scattering can be treated in a manner analogous to πd scattering, i.e., the IA can be formulated along with various types of corrections. From a practical standpoint, however, there are some difficulties. First, higher-order multiple (as well as double) scattering will play a significant role in K^-d reaction processes. This is because the K^-N scattering lengths are comparable to the internucleon distance of a deuteron. Second, the neglect of nucleon recoil during collision, which is a reasonable approximation in the πd case, may not now be valid because the kaon mass is larger than that of the pion. Third, there is no way at the present time of carrying out a detailed check of any theory due to the lack of availability of experimental data.

If we compare the various theories that have been proposed, we see that they differ from one another essentially in the way in which the multiple-scattering corrections to the IA are formulated. Thus, some approaches[26] make use of Brueckner's t-matrix formalism, others[27,29] emphasize the recoil and binding corrections during multiple scattering by assuming a separable nuclear potential, and still others[28] have introduced the concept of the initial state interaction in terms of which all orders of multiple scattering can be included in closed form by treating the nucleons as infinitely heavy. If multiple-scattering effects are included, then all the predictions of the K^-d total elastic and inelastic cross sections agree qualitatively with one another and also with the Alvarez experiment. In particular, these results show that multiple-scattering corrections to the IA are significant in K^-d scattering.

So far we have reviewed the standard impulse-approximation approach to the πd and K^-d problems. The many calculations, with double or multiple scattering included, are in qualitative agreement with one another, but detailed comparison among them is difficult because each one uses a different specific model. To remedy this point, and generally to bring the discussion into clear contact with modern dispersion theory, Brehm and Sucher[30] have studied the analyticity properties of πd elastic scattering with the aid of box diagrams. Such diagrams may be described as corresponding to processes in which the deuteron breaks up into two nucleons, the incident π meson interacting with one nucleon, after which the deuteron is formed again; this constitutes what we may term the dispersion-theoretic impulse approximation. Brehm and Sucher used a two-pole model which was adjusted so as to reproduce the features of elastic πN scattering, notably, the N^* p-wave resonance.

The πd scattering amplitude, when expressed as an integral over the relative momentum of the two nucleons, contains the πN amplitude in the integrand. Therefore, the πN amplitude is not on the energy shell in general. Defining the πN amplitude off the energy shell requires that one assume a certain form for the πN interaction off the energy shell, and this has always been a weak point of the standard impulse-approximation approach. In a dispersion-theoretic treatment of πd scattering, however, the πN amplitude off the energy shell follows from its analyticity properties.

The result of Brehm and Sucher was to find an angular distribution at 85 MeV which, despite the completely different approach, agrees fairly closely with that obtained by Rockmore (there is more backward scattering in the former case). We have already noted that multiple-scattering and binding (or potential) corrections are important in πd scattering. To incorporate these into dispersion theory is difficult because three-body and four-body intermediate states occur. The primary aim of this paper is to discuss such corrections without getting involved in the full complexity[31] of five- and six-point functions; this goal may be achieved by taking advantage of the fact that the deuteron is after all a simple system, and by being selective with respect to the choice of diagrams (the presence or absence of nearby singularities can be used to gauge the importance of a given diagram in the usual way[32]).

The first dispersion-theoretic approach to the πd scattering problem was attempted by Kaschluhn[33] who considered the forward elastic scattering. His purpose was to relate the forward scattering amplitude to experimentally measurable quantities; his method is analogous to the case of πN scattering.[34-36] While Kaschluhn asserts that the dispersion relation which he derived is consistent with the usual impulse approximation,[16] from a practical standpoint, however, this relation does not readily lend itself to a precise analysis of the πd problem. As in the case of πN scattering,[37] one can express the πd scattering amplitude as an analytic function of both s (the square of the total energy in the center-of-mass system) and t (the square of the momentum transfer in this system), but any discussion of multiple scattering or binding corrections requires the introduction of many-body intermediate states along with the rather involved integral equations which couple these various states. In point of fact, the success of the (Mandelstam) approach, where the amplitude in question is an analytic function of two variables, when applied to πN,[37] $\pi\pi$,[38] or other elementary processes[39] is due mainly to the fact that in these cases it is reasonable to assume that one has only two-body intermediate states.

If the (intermediate) states include more than two particles, complexities appear both in the kinematics and in the analyticity. The unitarity relation, which determines the discontinuity of an amplitude on the real axis of the s or t plane, also takes on an untractable form.[40,41] Cutkosky[40] has suggested a method for handling the unitarity relation in these cases, viz., that one find the discontinuity of an amplitude by replacing all the internal propagators in the corresponding Feynman diagrams with their momentum-conserving propagators (δ-function factors).

In the Mandelstam formulation of dispersion theory,[42] the amplitudes are represented in terms of spectral functions, which may in turn be expressed as integrals over the momentum variables of the intermediate states. In general these integrals will involve complex values of the virtual momenta. The application of Cutkosky's unitarity prescription to the case where one has only two-particle intermediate states is straightforward, and indeed one obtains the usual unitarity statement;[43] this is because any virtual momentum is completely determined by the δ-function factors (as in a box diagram). On the other hand, when one has multi-particle states (more than two particles), the regions of integration become undefined and the integrals for the spectral functions become meaningless. To remedy this difficulty, the usual procedure[44,45] is to define the region of integration by analytic continuation of the unitarity condition. This program has been carried out for a simple diagonal-type diagram by Gribov and Dyatlov.[46] Their result is rather difficult to generalize, and in any event this procedure is far from practical since the integration region will depend critically on the detailed analyticity properties of the particular amplitude. In fact, this is why Brehm and Sucher[30] had to confine their attention to simple box diagrams, which have only two-particle intermediate states.

It is evident that the general treatment of amplitudes with multi-particle intermediate states is very difficult. We can nonetheless make some progress if we limit ourselves from the very beginning to deuteron reactions. In the case of πd elastic scattering, for example, one can by physical arguments pick out a relatively small number of Feynman diagrams which still include many-particle intermediate states. It is then an essential point of this paper that these selected states can be reduced effectively to a superposition of two-particle states, in which case the usual unitarity relation may be applied.

Once the discontinuties of an amplitude are determined in this way, the assumption of analyticity immediately allows us to write down the dispersion relation for the amplitude. In our particular problem, it is important that the deuteron is not a simple elementary particle but rather the loosely bound state of a proton and neutron. In the language of dispersion theory, this implies the appearance of anomalous thresholds[47] in certain reactions involving the deuteron, an anomalous threshold consisting of a discontinuity below the normal threshold of the reaction determined from invariance considerations. This presents an additional complication which may, however, be handled by analytic continuation with respect to the deuteron mass. This procedure is particularly useful when the selected intermediate states lead to anomalous thresholds far below the normal ones. Then, so far as low-energy phenomena are concerned, the contribution from the normal region can be considered very small, while the details of the anomalous region must be carefully examined. The πd elastic-scattering amplitude has just this property. If an anomalous threshold is close to the normal threshold, then the contribution from the normal region has to be examined as well. This happens in fact in the case of $\bar{K}d$ scattering due to the larger mass of the $\bar{K}$ meson.

We begin the detailed exposition of this paper with some kinematical considerations in Sec. II. The invariants s, t, and u are introduced, and various kinematical quantities, such as momentum, energy, scattering amplitude, and scattering cross section, are expressed in convenient forms. The general analytic structures of the πd and $\bar{K}d$ scattering amplitudes are studied in Sec. III. There, the intermediate states are limited to two-body states, and the various box-type diagrams are examined as to the existence and behavior of their singularities. Anomalous thresholds appear in some cases and their structures are analyzed.

Our main problem is to treat the three-body intermediate states; accordingly, Sec. IV begins with a consideration of the multi-particle unitarity relation. Since the general analyticity properties of the amplitudes for the case of multi-particle intermediate states are complicated, mostly because of the involved kinematics, we confine ourselves to several simple diagrams which seem to be important on physical grounds, and study the analyticity properties of the corresponding amplitudes in detail. We encounter two types of diagram in this work, viz., triangle and (so-called) reduced box diagrams. For these cases, we can define the impulse approximation as well as binding and multiple-scattering corrections. After some approximations, we are able to calculate the discontinuity of an amplitude in the crossed channels when the deuteron mass is assumed small; with this result, we can immediately write down the dispersion relation for fixed s. Since this relation is valid for a fictitious deuteron mass and for an unphysical s value, we need to use a process of analytic continuation to obtain a result which holds in the physical region and for a real deuteron. In the course of the analytic continuation, we encounter anomalous thresholds and complex singularities. All of these questions are studied in Secs. IV and V for the triangle and the box diagrams, respectively.

Numerical results are given for πd elastic scattering in Sec. VI; here, it is the anomalous thresholds which play an important role. In Sec. VII, the case of $\bar{K}d$ scattering is treated in a similar manner, but now the situation is more complicated (as discussed previously). Only the impulse approximation is calculated numerically. We draw some conclusions about the usefulness of our overall approach in the concluding section.

II. KINEMATICS

In this section we shall define and explore some of the properties of several kinematical quantities which will be needed subsequently. Consider a scattering (or more generally, a reaction) involving two incoming particles having the mass values m_1 and m_2, respectively. The number of final particles is assumed to be two, with masses m_3 and m_4. This scattering phenomenon is completely described if the momenta, energies, and other quantum numbers (such as the spin) of the incoming and outgoing particles are specified, and may be pictured schematically as shown in Fig. 1. The shaded area represents any intermediate state which is compatible with the conservation of the relevant quantum numbers (e.g., baryon number, isotopic spin, strangeness, energy, etc.). The four-momentum of the *i*th particle is denoted by p_i, with all other quantum numbers indicated collectively by α_i. In point of fact, we shall consider only spinless particles hereafter, although the inclusion of spin is fairly straightforward, at least from a formal point of view.

It is well known[32,48] that the two-body scattering amplitude can be specified by two independent scalars. The usual choice is to define s, t, and u as follows:

$$\begin{aligned} s &= (p_1 + p_2)^2 = (p_3 + p_4)^2, \\ t &= (p_1 - p_3)^2 = (p_2 - p_4)^2, \qquad (2.1) \\ u &= (p_1 - p_4)^2 = (p_2 - p_3)^2, \end{aligned}$$

where s, t, and u are not independent but are related, viz.,

$$s + t + u = \sum m_i^2. \qquad (2.2)$$

Consider once again Fig. 1, which represents six reactions as shown.

We define the s, t, and u channels by pairing particles—two incoming and two outgoing—in the usual way.[32] In the s channel, for example, with E the total energy and θ the scattering angle between 1 and 3 in the barycentric system, we have

$$
\begin{aligned}
s &= (p_1+p_2)^2 = (p_{10}+p_{20})^2 - (\underset{\sim}{p_1}+\underset{\sim}{p_2})^2 = E^2, \\
t &= (p_1-p_3)^2 = m_1^2 + m_3^2 - 2p_{10}p_{30} + 2|\underset{\sim}{p_1}||\underset{\sim}{p_3}|\cos\theta, \qquad (2.3) \\
u &= (p_1-p_4)^2 = m_1^2 + m_4^2 - 2p_{10}p_{40} - 2|\underset{\sim}{p_1}||\underset{\sim}{p_3}|\cos\theta,
\end{aligned}
$$

where $\underset{\sim}{p}_i$ indicates the three-momentum of the ith particle. If $m_1 = m_3$, $m_2 = m_4$, and if $|\underset{\sim}{p}_1|$ is denoted by p, we obtain

$$
\begin{aligned}
s &= E^2, \\
t &= -2p^2(1-\cos\theta), \qquad (2.4) \\
t &= -2p^2(1+\cos\theta).
\end{aligned}
$$

If in any channel (say, the s channel) the corresponding two reactions are energetically accessible, the invariants assume "physical" values in this channel; it is then obvious that s > 0, t $\leq$ 0, and u $\leq$ 0. The physical values of the invariants in each channel can be determined easily. Suppose, for example, that in Fig. 1, m_1 and m_3 are pions, and m_2 and m_4 are deuterons. Then the s channel corresponds to πd elastic scattering, i.e., $\pi d \to \pi d$, the t channel to $\pi\bar{\pi} \to d\bar{d}$, and the u channel to $\bar{\pi}d \to \bar{\pi}d$. The physical values of s and t (hence also u) in the s channel are determined from the conditions,

$$
\begin{aligned}
s &\geq (m_1+m_3)^2 = (\mu+d)^2, \qquad (2.5) \\
-1 &\leq \cos\theta \leq 1,
\end{aligned}
$$

where μ and d are the masses of the pion and deuteron, respectively. The corresponding area of the real s,t plane is shaded in Fig. 2 and is there denoted by s. The physical values of the invariants in the t and u channels can be determined in a similar manner, and are also shown in Fig. 2.

The scattering amplitude in any channel is a function of s, t, and u. To relate the amplitudes for the various channels to one another, Chew[32] has emphasized the important role of the substitution law. According to this law, the amplitude in the s channel has the same analytic form as that in the t channel, but since the physical values of the invariants in the s channel will not overlap those of the t channel, we need a process of analytic continuation in order to find the physical amplitude in the one channel from a knowledge of the physical amplitude in the other.

Now we define the T matrix (the invariant scattering amplitude) in terms of the S matrix,[48] viz.,

$$\langle f|S|i\rangle = \langle f|i\rangle - (2\pi)^4 i\,\delta^4(P_f - P_i)\langle f|T|i\rangle, \tag{2.6}$$

where $|i\rangle$ is the initial state in the Heisenberg representation (expressed in terms of the "in" or "out" basis) with the total momentum P_i, and $|f\rangle$ is the final state with the total momentum P_f. We adopt here a form of covariant normalization[48] which implies the following completeness property of the states:

$$1 = |0\rangle\langle 0| + \int\frac{d^4k}{(2\pi)^4}|k\rangle 2\pi\delta(k^2-m^2)\theta(k_0)\langle k|$$

$$+ \int\frac{d^4k_1}{(2\pi)^4}\frac{d^4k_2}{(2\pi)^4}|k_1 k_2\rangle 2\pi\delta(k_1^2-m_1^2)\theta(k_{10})2\pi\delta(k_2^2-m_2^2)\theta(k_{20})\langle k_1 k_2| + \cdots \quad ; \tag{2.7}$$

$k, k_1, k_2, \cdots$ are four-momenta, and $\theta(k_o)$ is the step function, i.e.,

$$\theta(k_o) = 1, \qquad k_o > 0,$$
$$= 0, \qquad k_o < 0.$$

We can express the scattering cross section in terms of the T matrix. Consider the scattering of two spinless particles. Suppose the initial state $|i\rangle$ is $|p_1 p_2 \text{ in}\rangle$ and the final state $|f\rangle$ is $|p_3 p_4 \text{ in}\rangle$ and let $\langle f|T|i\rangle$ be denoted by T_{fi}. The density of the final states ρ_2 will then be given by

$$\rho_2 = 2\pi\delta(p_3^2 - m_3^2)\theta(p_{30})2\pi\delta(p_4^2 - m_4^2)\theta(p_{40})(2\pi)^4\delta^4(P_f - P_i)\frac{d^4p_3}{(2\pi)^4}\frac{d^4p_4}{(2\pi)^4}. \tag{2.8}$$

In the center-of-mass system,

$$\rho_2 = \frac{1}{16\pi^2}\frac{|\underset{\sim}{p}_f|}{E}\, d\Omega_c \; , \tag{2.9}$$

where $\underset{\sim}{p}_f$ is the momentum of one of the final-state particles, E is the total energy of the system, and $d\Omega_c$ is the element of solid single associated with $\underset{\sim}{p}_f$. Using the above relations, one finds for the differential scattering cross section the expression

$$\frac{d\sigma}{d\Omega_c} = \frac{|\underset{\sim}{p}_f|}{|\underset{\sim}{p}_i|}\left|\frac{T_{fi}}{8\pi E}\right|^2 , \tag{2.10}$$

where $\underset{\sim}{p}_i$ is the corresponding momentum for the initial state. In comparison with the results of potential theory, we see that T_{fi} is related to the (non-invariant) scattering amplitude f_{fi} by

$$f_{fi} = -\left(T_{fi}/8\pi E\right). \tag{2.11}$$

The S matrix is unitary, i.e., it satisfies

$$S^\dagger S = I .$$

If we take a matrix element between an initial state and a final state, this relation becomes, in terms of the T matrix,

$$(T - T^{\dagger})_{fi} = -i \sum_{n} (T^{\dagger})_{fn} (2\pi)^4 \delta^4(P_n - P_i) T_{ni} \, ,$$

or

$$T_{fi} - T_{if}^{*} = -i \sum_{n} T_{nf}^{*} (2\pi)^4 \delta^4(P_n - P_i) T_{ni} \, . \tag{2.12}$$

In the right-hand side of Eq. (2.12) we sum over all intermediate states* n which have the same total four-momentum P_n as both the initial and the final states, and which are allowed by the various other conservation laws.

Consider the two-body intermediate states in particular. Let $P_i^2 = s$, and express the right-hand side of Eq. (2.12) in terms of s; we have

$$-\frac{i}{16\pi^2} \frac{Q(s; m_1 m_2)}{\sqrt{s}} \int d\Omega \, T_{nf}^{*} T_{ni} \, \theta(s - (m_1 + m_2)^2) \, , \tag{2.13}$$

where

$$Q(s;m_1 m_2) = \frac{1}{2\sqrt{s}} [s-(m_1+m_2)^2]^{1/2} [s-(m_1-m_2)^2]^{1/2} \tag{2.14}$$

is the magnitude of the momentum of one of the particles in the center-of-mass frame, and dΩ is the element of solid angle associated with $\underset{\sim}{Q}$.

*The state n will be called an intermediate state whether the particles in the state are on the mass shell or not.

III. THE ANALYTICITY PROPERTIES OF THE SCATTERING AMPLITUDES

In this section, we confine ourselves to the study of the analyticity properties of the two-body scattering amplitudes with the intermediate states limited to two-body states. As discussed in the previous section, the scattering amplitudes in this case are completely specified by any two invariants among the three quantities s, t, and u. Our study here is concerned with locating and describing the singularities of the invariant amplitude T, defined in the preceding section, considered as a function of two complex variables.

In the consideration of the analyticity of the scattering amplitude, there are two different approaches: the derivation of the dispersion relation from axiomatic field theory,[49-53] and from perturbation theory.[54,57] Attempts to deduce analyticity properties from axiomatic field theory meet up with considerable difficulty, whereas in perturbation theory each term of the expansion corresponds to a Feynman diagram and the analytic continuation can be carried out comparatively easily for each such diagram. For the derivation of a dispersion relation, it is essential to know the location of the singularities (poles and branch points) of the amplitude and the values of the discontinuities of the amplitude across the branch cuts associated with the branch points. Perturbation theory provides a clear answer to this problem. Furthermore, it has been shown in perturbation theory[40,42] that the discontinuities across the cuts can also be calculated by applying the unitarity of the S matrix to the scattering amplitude; this leads to Chew's conjecture[32] that the amplitude is analytic in a cut plane (complex plane with poles and branch cuts) where the cuts are only those required by unitarity.

This assumption is a guiding principle in studying the analyticity of amplitudes, especially when the Mandelstam representation is not valid, as will be shown later for the case of πd and $\bar{K}d$ scattering.

We proceed to examine the singularities of the πd and $\bar{K}d$ amplitudes using perturbation theory. A scattering amplitude corresponding to a Feynman diagram can be expressed as an integral over the internal momenta and is a function of the external momenta. General conditions concerning the existence of the singularities of such functions defined by multiple integrals have been examined by several authors.[54,58,59] It is found that for a multiple integral to be singular it is necessary that it have either

(i) an end-point singularity, or

(ii) coincident singularities which pinch the contour at every stage of the integration.

This condition has been applied to the study of the analyticity of Feynman diagrams by Landau,[60] Bjorken,[61] and Cutkosky.[40]

Consider a general Feynman integral expressed in the form

$$F_\varepsilon = \int d^4k_1 \cdots d^4k_\ell \, \frac{B}{\prod_1^n (q_i^2 - m_i^2 + i\varepsilon)} \,, \quad \varepsilon > 0 \,, \tag{3.1}$$

where q_i denotes the four-momentum of the ith propogator of the Feynman diagram, m_i is the corresponding mass, and B is a constant. The variables k_i are the four-momenta associated with the ℓ independent loops of the diagram, which variables k_i can be chosen arbitrarily except that they must be consistent with momentum conservation. Here we assume that all particles are bosons for the sake of simplicity. (No new difficulties arise from the introduction of Fermi particles.) The scattering amplitude in the physical region of the external momenta is given by

$$F = \lim_{\varepsilon \to 0} F_\varepsilon \,.$$

The singularities of F_ε in the limit $\varepsilon \to 0$ can be found in the following ways (these are the so-called Landau-Cutkosky rules[40,60,61]):

(a) Either they already appear as singularities of the reduced diagrams of F_ε (where the reduced diagrams are derived from the original diagram corresponding to F_ε by contracting the internal lines (see, e.g. Fig. 3);

(b) or they are <u>leading</u> singularities, i.e., they are not contained in the reduced diagrams. These may be found by imposing the mass-shell conditions

$$q_i^2 = m_i^2, \quad i = 1, \cdots, n \tag{3.2}$$

on the set of equations

$$\sum \alpha_i q_i = 0 \tag{3.3}$$

(where one has one such equation for each independent loop of the diagram), and then searching for the q_i's which lead to non-negative α_i's.*

Equation (3.3) is equivalent to the form det $(q_i q_j) = 0$, where, evidently, for a given independent loop, $\underline{i}$ and $\underline{j}$ can assume only the values appropriate to the loop. By way of example, the leading singularities of the box diagram of Fig. 3a can be found from

$$\det(q_i q_j) = 0, \quad i,j = 1, \cdots, 4, \tag{3.3a}$$

plus the four mass-shell conditions; the (remaining) singularities may be determined by equating the principal minors to zero and imposing the appropriate mass-shell conditions, etc.

---

*The corresponding singularities lie in the physical sheet.

Now it has been shown[54] that the physical scattering amplitude $F(s,t)$ corresponding to a given Feynman diagram is a boundary value of an analytic function $F(z,t)$ approaching the positive real s axis from above, with t fixed and negative. On the other hand, if T_{fi}, the invariant scattering amplitude, is the boundary value of an analytic function of complex s and of fixed negative t, approaching the real s axis from above, then T^*_{if} is the boundary value of the same anslytic function approaching the s axis from below.[62-64] This implies that, if T_{fi} is identified with $F(s+i\varepsilon,t)$, then T^*_{if} corresponds to $F(s-i\varepsilon,t)$. Therefore, the difference $T_{fi}-T^*_{if} = F(s+i\varepsilon,t)-F(s-i\varepsilon,t)$ expresses the discontinuity of $F(z,t)$ across a branch cut on the positive real s axis for fixed negative t. If $F(z,t)$ is real on some section of the real s axis, then the discontinuity of $F(z,t)$ across the branch cut equals $2i\mathrm{Im}\, F(s+i\varepsilon,t)$. This has been proved[62] for any two-particle scattering amplitude (with or without spin) both in perturbation theory and in the LSZ formulation. In the latter case, the TCP theorem plays a key role.

It is evident that the unitarity relation (2.12) expresses the discontinuity of the scattering amplitude across a branch (unitarity) cut. One may next conjecture[32] that the singularities of the scattering amplitude are only those required by unitarity. In perturbation theory, one can show that the Landau-Cutkosky rules follow from unitarity.[43]

We next consider the particular processes of πd and $\bar{K}d$ elastic scattering; these are shown symbolically up to four-body intermediate states in the t or u channel in Fig. 4 (no process corresponding to three-meson intermediate states is listed due to conservation of G parity). A blob is used to represent the various ways in which the particles emanating from the blob can interact. For instance, Fig. 4a includes, among other possibilities, those shown in Fig. 5. Figure 5a corresponds to πd ($\bar{K}d$) elastic scattering, where the incoming deuteron breaks up into two nucleons, one of which absorbs the incoming $\pi(\bar{K})$, then emits the outgoing $\pi(\bar{K})$, and finally interacts with the other nucleon to form the outgoing deuteron. The intermediate state in the s channel for this case consists of two nucleons (a nucleon and a hyperon). Figure 5b can be similarly interpreted except that the intermediate state in the s channel now consists of one nucleon plus a πN (πY(hyperon) or $\bar{K}N$) scattering state. If we study Figs. 5c and 5d in terms of u and t, the analyses of Figs. 5a and 5b, respectively, can be applied directly in these cases except that s is replaced by u.

The singularities of the scattering amplitude corresponding to Fig. 4a have been studied by many authors[30,59,65] and will be described for πd and $\bar{K}d$ scattering in what follows.

Consider first πd elastic scattering of the type shown in Fig. 5a. The Landau-Cutkosky analysis (see Fig. 3a) is directly applicable in this case. The normal threshold* in the s channel is $4M^2$; it is again $4M^2$ in the t channel (M is the nucleon mass). These singularities correspond to $\alpha_2 = \alpha_4 = 0$, and $\alpha_1 = \alpha_3 = 0$, respectively. To study the possibility of anomalous thresholds,[65,66] we draw the reduced diagrams of Fig. 5a in which only one of the α_i is zero. These are given in Figs. 6a, 6b, and 6c, corresponding to $\alpha_3 = 0$, $\alpha_1 = 0$, and $\alpha_4 = 0$, respectively. The figure which is not shown here, corresponding to $\alpha_2 = 0$, has the same analytic properties as Fig. 6c. The duals[54,60,67] of Figs. 6a, 6b, and 6c are shown in Figs. 6a', 6b', and 6c', respectively.

---

*The normal threshold for a given diagram in the s channel, say, is defined as the smallest energy of the allowable intermediate states. It can be shown from unitarity that the normal threshold occurs as a branch point of the scattering amplitude on the real s axis. Other singularities on the real axis which are produced by the unitarity integral (right-hand side of Eq. (2.12)) are termed anomalous.

Since the duals 6a' and 6c' are triangles, there will be anomalous thresholds in the t as well as the s channel for πd scattering of the type given in Fig. 5a. These are denoted by t_o and s_o, respectively, and lie in the physical sheet. On the other hand, the dual 6b' corresponding to Fig. 6b will not form a triangle, and t_o' is therefore not a singular point in the physical sheet. From geometry, we have

$$\begin{aligned} t_0 &= 4d^2 - d^4/M^2 \simeq 1.73\mu^2 , \\ t_0' &= 4\mu^2 - \mu^4/M^2 , \\ s_0 &= d^2 + \mu^2 - \frac{\mu^2 d^2}{2M^2} + 2\mu d\sqrt{\left(1-\frac{d^2}{4M^2}\right)\left(1-\frac{\mu^2}{4M^2}\right)} . \end{aligned} \tag{3.4}$$

The Landau curve $t = t(s)$ is determined from Eq. (3.3a),

which reduces to the two equations,

$$t = 4M^2 \frac{(s-s_0)(s-s_0')}{s(s-4M^2)} , \tag{3.5}$$

and

$$t = 0,$$

where

$$s_0' = d^2 + \mu^2 - \frac{\mu^2 d^2}{2M^2} - 2\mu d\sqrt{\left(1-\frac{d^2}{4M^2}\right)\left(1-\frac{\mu^2}{4M^2}\right)} . \tag{3.6}$$

The solution $t = 0$ does not correspond to a singularity in the physical sheet. The Landau curve is shown in Fig. 7a.

The part of the curve for which $s > 4M^2$ and $t > 0$ lies in the physical sheet. Since s_o' is not in the physical sheet, the same must hold for points on the Landau curve with $s < s_q$. As s increases, s reaches s_q at which point $t = t_o$ (or $\alpha_3 = 0$). As s increases further, points on the curve correspond to $\alpha_3 > 0$, so that the portion of the curve with $s_q < s < 4M^2$ is in the physical sheet. For $t_o < t < t_o'$, s becomes complex on the Landau curve and the Mandelstam representation is not valid in this case.[40] But as long as s is real, t(s) is real, so that a dispersion relation in t with s fixed and real would appear to be more convenient than one in s with fixed t.

A similar technique can be applied to Fig. 5b,* where the meson is rescattered by the same nucleon, so that meson-baryon scattering states are included in the intermediate state. The Landau curve for this case is shown in Fig. 7b. Now we have an anomalous threshold in the t channel in the physical sheet, but not in the s channel. Other anomalous thresholds appear in the unphysical sheets. Note also that t_o lies in the physical region of s, i.e., $s \geqslant$ (normal threshold in s) = $(2M+\mu)^2$.

The same procedure can be applied to $\bar{K}d$ scattering. In the process corresponding to Fig. 5a, the meson line now refers to the $\bar{K}$ particle, and the baryon which absorbs and emits the meson will now be a hyperon with mass Y (the masses corresponding to specific hyperons will be denoted by the particle symbols themselves). If the hyperon is Λ, Σ, or Y_o^* (1403), we have anomalous thresholds in both the t and s channels. The Landau curve for this case is shown in Fig. 7a'. The magnitude of t_o is the same as in the πd case, whereas t_o' and s_o are different; these statements may

---

*As far as the singularities of the amplitude are concerned, this diagram is essentially the same as the box diagram, so that the Landau-Cutkosky rules for the box diagram can be applied here.

be easily verified by inspection of the duals. If the hyperon is Y_o^* (1520), then only the anomalous threshold in t appears in the physical sheet, and the Landau curve looks like Fig. 7b.

We turn next to a consideration of the process given in Fig. 5b applied to $\bar{K}d$ scattering. The (meson-baryon) scattering intermediate state will now involve either $\bar{K}N$ or $\pi\Lambda$ $(\pi\Sigma)$. Because of the mass difference between the $\bar{K}N$ and πY systems, the process with the $\bar{K}N$ scattering state has an anomalous threshold (in t in the physical sheet), while that process with the πY scattering state has anomalous thresholds in both s and t. The Landau curve for the former case is like that of Fig. 7b, while the curve for the latter case resembles Fig. 7a'. Generally, as the internal masses become larger, the curves become more "normal."[42]

IV. A SIMPLE MODEL--TRIANGLE DIAGRAMS

We now consider scattering amplitudes with many-body intermediate states. Let us first rewrite the unitarity relation, Eq. (2.12), in a form which will prove useful for our present purposes. We consider here again the scattering of two particles. The contribution of the three-body states to the right-hand side of (2.12) is

$$-i\int \frac{d^4q_1\, d^4q_2\, d^4q_3}{(2\pi)^9}\, \delta(q_1^2-m_1^2)\,\delta(q_2^2-m_2^2)\,\delta(q_3^2-m_3^2)\,\theta(q_{10})\,\theta(q_{20})\,\theta(q_{30})$$
$$\times(2\pi)^4\delta(q_1+q_2+q_3-p_i)\, T_{3f}^{*}\, T_{3i}\,. \qquad (4.1)$$

As in the case of the two-body intermediate states, some of the q_i integrations can be readily performed. For this purpose, we introduce new variables to specify the configuration of the three-body system.

We define the direction of $\underset{\sim}{q}_3$ by the two angles $\Omega = (\theta,\phi)$ measured with respect to a given reference frame in the three-body center-of-mass system. In this system the direction of $\underset{\sim}{q}_1+\underset{\sim}{q}_2$ is opposite to that of $\underset{\sim}{q}_3$, but the relative orientation of $\underset{\sim}{q}_1$ and $\underset{\sim}{q}_2$ has yet to be specified. Towards this end, we designate the direction of $\underset{\sim}{q}_1$ by $\Omega' = (\theta',\phi')$ measured with respect to a set of coordinate axes in the rest frame of the 1,2 pair. In addition, we define the invariant variable ξ by $\xi = (q_1+q_2)^2$. The variables Ω, Ω', ξ together with $s = (q_1+q_2+q_3)^2$ will then describe the configuration of the three-body system completely.

In terms of these variables, the expression (4.1) becomes

$$-2\pi i\int d\Omega\, d\Omega'\, d\xi\, \rho(s;\sqrt{\xi}, m_3)\,\rho(\xi;m_1 m_2)\, T_{3f}^{*}\, T_{3i}\,, \qquad (4.2)$$

where

$$\rho(s;m_1 m_2) = \frac{1}{(2\pi)^3}\,\frac{1}{4\sqrt{s}}\, Q(s;m_1 m_2)\,\theta(s-(m_1+m_2)^2)\,.$$

Q is given explicitly by Eq. (2.14).

As in the case of scattering amplitudes with two-body intermediate states, the analyticity properties of the amplitudes with many-body intermediate states can be studied with the help of the Landau-Cutkosky rules. Now, however, the algebra becomes far more complicated except when we have simple relations among the masses.[46,68,69] This is precisely the difficulty which the analysis of πd and $\bar{K}d$ scattering with many-body intermediate states faces. If we confine ourselves to two-body states only, however, the method is useful to determine the location of the singularities of the amplitudes. Can the analyticity of the πd and $\bar{K}d$ scattering amplitudes with many-body intermediate states be determined without getting into all the aforementioned complications?

Our ultimate aim is to determine a scattering amplitude as an analytic function of invariants (s,t, and u) which satisfies the unitarity relations in the s,t, and u channels. One way[32] to solve this problem is to decompose the scattering amplitude into its partial amplitudes (amplitudes for precise angular-momentum states) and then to determine each partial amplitude by means of a set of (integral) equations for each angular-momentum state. This method has been widely used[32,37-39] in the study of elementary-particle interactions.

The application of a partial-wave analysis to the πd and $\bar{K}d$ problems leads to serious difficulties, however: elastic unitarity cannot be used even at low energy, the many-body intermediate states must be taken into account seriously,[27-29] and the left-hand cuts which are associated with the reactions in the crossed channels have to be found. To formulate the integral equations for the partial amplitudes of πd and $\bar{K}d$ scattering, one would have to solve these difficulties first.

Instead, we attack the πd and $\bar{K}d$ problems from a different point of view. The generalized Feynman diagrams which contribute to the elastic scattering have already been given symbolically in Fig. 4. We undertake a more systematic study of these diagrams now, noting that in these diagrams each blob includes many kinds of complicated interactions. Corresponding to Fig. 4a, for example, some of the possibilities which the lower blob represents are shown in Figs. 8a - 8d. Here, the horizontal broken lines indicate the particles which are in the intermediate states in the t channel. The intermediate states are common in these four diagrams, and are the two-nucleon states. The normal thresholds of the amplitudes have a common value in the t channel, i.e., $t = 4M^2 = 180.8\mu^2$. The other internal lines may be regarded as contained in the T_{fn} or T_{ni} for the t channel.

If we put aside the question of anomalous thresholds for the moment, then, so long as the intermediate states are the same, so that the normal thresholds are the same, no one particular diagram is obviously more important than any other diagram in describing the reaction in the t channel ($d\bar{d} \to \pi\bar{\pi}$, or $d\bar{d} \to K\bar{K}$). However, when there are anomalous thresholds due to the specific interactions which the blobs in Fig. 4a represent, the situation may become different. In order to find out whether and where the anomalous thresholds appear, we shall use the technique of dual diagrams.[65,67]

The reduction of box diagrams to triangle diagrams has already been described in Sec. III (see Figs. 5 and 6). We can reduce the diagrams in Fig. 8 in a similar fashion. By contracting the upper blob (a function of two variables) of each diagram to a vertex (a function of one variable), we obtain the corresponding triangle diagrams.

The anomalous threshold t_0 in the t channel corresponding to Fig. 8a may be obtained by a simple geometrical consideration. The result, which includes the general case where the mass of the horizontal propagator is m_1 and the masses of the intermediate states are m_2 and m_3, is

$$t_0 = \frac{1}{4m_1^2}\left[\Delta(m_1 m_2) + \Delta(m_1 m_3)\right]^2 + \frac{(m_2^2 - m_3^2)^2}{4m_1^2}, \quad (4.3)$$

where

$$\Delta(m_1 m_2) = \Delta(m_2 m_1) = \left\{\left[(m_1+m_2)^2 - d^2\right]\left[d^2 - (m_1-m_2)^2\right]\right\}^{1/2}.$$

Upon setting $m_1 = m_2 = m_3 = M$ in the above equation, we obtain

$$t_0 = 4d^2 - d^4/M^2 \approx 1.73\mu^2.$$

This value is evidently small compared to the normal threshold $180.8\mu^2$. If, instead, we set $m_1 = M+\mu$ and $m_2 = m_3 = M$ in Eq. (4.3) (corresponding to Fig. 8b), we have

$$t_0 = \frac{1}{(M+\mu)^2}\left[(2M+\mu)^2 - d^2\right]\left[d^2-\mu^2\right],$$

which, as a function of μ, increases rapidly as μ increases. Numerically, $t_0 \approx 110\mu^2$. Finally, one may determine the t_0's corresponding to Figs. 8c and 8d, viz.,

$$t_0 = 27\mu^2, \qquad \text{for Fig. 8c};$$

$$= 83\mu^2, \qquad \text{for Fig. 8d}.$$

As we have just seen, the anomalous thresholds which are obtained for the several representations of Fig. 4a are always smaller than the normal threshold. This means that the branch cut in the t channel must be extended below the normal threshold, $4M^2$, down to the lowest of the t_o's. If the reaction in the s channel is at low energy, we expect, in view of the dependence of t on energy and angle (Eq. (2.4)), that the contribution to the scattering amplitude from those diagrams which have smaller anomalous thresholds will dominate and that the approximation in which we select only a few diagrams will be justified. On this basis, the contribution of Fig. 8a to the two-body intermediate-state term in Eq. (2.12) is clearly dominant over those of Figs. 8b - 8d and the scattering amplitude corresponding to this diagram can be expected to be a good approximation to the elastic scattering (the principle of "nearby" singularities).[32]

As in the case of the potential theory of πd and $\bar{K}d$ scattering, we can define the impulse approximation, binding corrections to the impulse approximation, double scattering, and multiple scattering in terms of generalized Feynman diagrams. In fact, at low energy, there seems to be a close correspondence between potential theory and the relativistic dispersion-theoretic approach.[70,71]

For the sake of simplicity, we shall limit our considerations to triangle diagrams for the remainder of this section. We define the impulse approximation for πd or $\bar{K}d$ scattering as the amplitude corresponding to Fig. 8a, neglecting the contributions of Figs. 8b - 8d since the latter have larger anomalous thresholds. In our definition of the impulse approximation, we do not specify the details of the πN or $\bar{K}N$ scattering amplitude (the vertex at the top of Fig. 8a), except to assume that it depends only on t. In the next section, we will extend the definition of the impulse approximation to the πd and $\bar{K}d$ scattering amplitudes when we have box diagrams; there, both the s and t dependences of the πN and $\bar{K}N$ interactions need to be taken into account.

By contracting the upper blob in Fig. 4b, we obtain a correction to the impulse approximation. Some of the resultant diagrams which have anomalous thresholds are shown in Figs. 9a and b, and the corresponding duals are given in Figs. 9a' and b', respectively. Evidently, we can take Fig. 9a as the leading binding correction to the impulse approximation. We note that the intermediate meson is a π meson in the $\bar{K}d$ as well as in the πd case. No binding correction due to K mesons is allowed, because of the conservation of strangeness.

Other corrections to the impulse approximation are obtained by contracting the upper blob of Fig. 4c. A resultant triangle diagram is shown in Fig. 9e; evidently, this case corresponds to a multiple (triple) scattering. For elastic πd scattering, the anomalous threshold for Fig. 9e is $28\mu^2$. In the $\bar{K}d$ case, the intermediate mesons can be two kaons (no anomalous threshold) or two pions (threshold at $28\mu^2$).

It is convenient to consider next the diagram shown in Fig. 4e. This diagram may be regarded as the process in which the incident meson is absorbed by the one nucleon and the outgoing meson is emitted by the other. Note that this diagram is drawn in the s and u channels. Evidently such a process exists only for πd scattering and not for $\bar{K}d$ scattering in view of strangeness conservation. Approximating the generalized interactions in T_{ni} and T_{nf} in the u channel with single nucleon lines, we obtain the anomalous threshold u_o,

$$u_o = d^2 + \mu^2 - \frac{\mu^2 d^2}{2M^2} + \frac{\mu d}{2M^2} \sqrt{(4M^2 - d^2)\ (4M^2 - \mu^2)} \approx 180.6\mu^2,$$

which is very near the normal threshold. Therefore the contribution of this diagram to πd scattering is expected to be small, and will not be considered further in this section.

The diagram shown in Fig. 4f may be considered as describing a correction to Fig. 4e. Some of its representations are shown in Figs. 9c and d. These diagrams correspond to double scattering (in both the πd and $\bar{K}d$ cases). The amplitude corresponding to Fig. 9d has no anomalous threshold, unlike that of Fig. 9c where the value of the threshold depends, of course, on the masses of the baryons and the mesons participating in the interaction. Our definition of double-scattering includes only Fig. 9c.

We consider next Fig. 4d, in which the intermediate state in the t channel consists of two mesons. Now the amplitude has no anomalous threshold, but the normal threshold is at $t = 4\mu^2$ for πd scattering and at $t = 49\mu^2$ for $\bar{K}d$ scattering. Therefore, this diagram should be important, especially for the study of πd scattering. If we try to take this diagram seriously, however, we have to deal with a set of integral equations involving at least the $d\bar{d} \to \pi\pi$, and $\pi\pi \to \pi\pi$ amplitudes, but this is beyond the scope of the present paper.*

To this point, we have surveyed all the diagrams shown in Fig. 4, and in particular, have classified the associated triangle diagrams according to the impulse approximation, binding corrections, double scattering, and multiple scattering. We consider next the analyticity properties of these amplitudes in more detail.

We begin with the unitarity relations (Eqs. (2.12) and (4.2)) applied to these amplitudes in the t or u channels. Suppose first that the deuteron mass is so small that no anomalous thresholds appear

---

*On replacing the upper blob of Fig. 4a by a two meson state (in the t channel) one can estimate part of the effect of the[30] $\pi\pi$ interaction on πd scattering; this effect turns out to be small.

in the channels in question.[44,45] In this case, the unitarity relation tells us that there exists a discontinuity of the amplitude across the unitarity cut above the normal threshold. We can then express each amplitude in terms of its discontinuity by the Cauchy integral theorem, yielding a dispersion relation. We assume that the amplitude goes to zero sufficiently rapidly at infinity. As the deuteron mass increases to its physical value, anomalous thresholds may appear and the form of the dispersion relation may have to be modified. We are most interested in which way the modification arises.

The rest of this section will be devoted to the study of the analyticity of the impulse-approximation and of the double-scattering amplitudes; for the sake of definiteness, $\bar{K}d$ scattering will be considered. It is rather straightforward to analyze the remaining amplitudes in view of the similarity of the triangle diagrams to the deuteron form factors.[71] We shall take up all these amplitudes again when we consider the more complicated diagrams in the next section.

The diagrams we study are those shown in Fig. 10. The scattering amplitude corresponding to $N\bar{N} \rightarrow K^+K^-$ will be denoted by $g(t)$, and that corresponding to $K^+d \rightarrow K^-NN$ by $G(u,\xi)$, where ξ is the sub-energy variable as used in Eq. (4.3). The quantity $\tilde{G}(u,\xi)$ represents $K^-NN \rightarrow K^+d$. The invariant x is defined in terms of the process $\bar{K}\bar{d} \rightarrow \bar{K}\bar{N}\bar{N}$ as the square of the momentum transfer in the center-of-mass frame of the total system (in the u channel), while v is the corresponding invariant in the ξ channel. We assume from now on that the scattering amplitude in question is represented by a real analytic function, so that the discontinuity across a cut on the real axis will be in its imaginary part.

Under these circumstances, it is easy to write down the discontinuities (the imaginary parts) of the impulse-approximation and the double-scattering amplitudes across the t and the u axes above the respective normal thresholds provided the mass of the deuteron is so small that there are no anomalous thresholds.

Consider first the impulse approximation (Fig. 10a). The momenta of the nucleon and the deuteron are shown in the diagram. Let $d\Omega$ be the element of solid angle associated with the three-momentum $\underset{\sim}{q}$ in the center-of-mass frame of the total system. If z_v is the cosine of the polar angle and ϕ is the azimuthal angle of $\underset{\sim}{q}$ in a reference frame with $\underset{\sim}{p}$ in the z direction, then $d\Omega = dz_v d\phi$. The momentum-transfer variable v is

$$v = (p-q)^2 = M^2 + d^2 - 2p_0 q_0 + 2|\underset{\sim}{p}||\underset{\sim}{q}|z_v .$$

The imaginary part of the scattering amplitude corresponding to the impulse approximation (Fig. 10a) then becomes, in view of Eq. (2.13),

$$-2\pi^2 \int_{-1}^{1} dz_v \frac{\rho(t;MM)\,\Gamma_0^{\,2} g(t)}{v - M^2} , \tag{4.4a}$$

where Γ_o is the coupling constant of the dNN vertex, and the ϕ integration has already been carried out. The $\rho(t;MM)$ is defined in conjunction with Eq. (4.2). Insofar as the dispersion relation in the impulse approximation is concerned, this can be deduced by the techniques to be developed in the remainder of this section; the result will be quoted later.

Now for the double scattering as shown in Fig. 10b, where the momenta of the internal particles are explicitly shown. It is convenient to specify the intermediate state in the u channel by means of the same variables (one sub-energy variable, four angular variables), as in deriving Eq. (4.2). The quantity v depends on the four masses, $m_K, M, \sqrt{x}$, and d, so that v will often be denoted by $v(\xi; m_K M \sqrt{x}\ d)$, where the propagator corresponding to x may be a hyperon with mass Y (not necessarily on the mass shell).

The imaginary part of the double-scattering amplitude can be written down, in view of Eq. (4.2), as

$$-\pi \int d\Omega\, d\Omega'\, d\xi\ \frac{G(u_-,\xi_-)\,\rho(u;\sqrt{\xi}M)\,\rho(\xi;M m_K)}{(x - Y^2)(v - M^2)} .$$

The notation $G(u_-,\xi_-)$ indicates that the amplitude is to be evaluated from below the u and ξ axes. The imaginary part of the double-scattering amplitude, denoted by Im $T_d(u)$, is then

$$\operatorname{Im} T_d(u) = -(2\pi)^2 \pi \int d\xi\, G(u_-,\xi_-)\,\rho(u;\sqrt{\xi}M) \int_{-1}^{1} dz_x \frac{1}{Y^2 - x}$$
$$\times \int_{-1}^{1} dz_v \frac{\rho(\xi; M m_K)}{M^2 - v}$$

$+$ a term with G replaced by $\tilde{G}$. (4.4b)

The z_v integral has the same form in (4.4a) and (4.4b). Thus, the right-hand side of (4.4b) includes an integral over the z_v associated with the circled part of Fig. 10b which can be regarded as the dYξ vertex (a function of ξ). This vertex has an anomalous threshold in ξ for the physical deuteron, as can be seen from its dual which is shown in Fig. 9c'.

The $dY\xi$ vertex $\Gamma_Y(\xi)$ is formally defined as the function of ξ whose imaginary part is given by

$$\mathrm{Im}\,\Gamma_Y(\xi) = 2\pi^2 \rho(\xi;Mm_K)\int_{-1}^{1} dz_v \frac{g\Gamma_0}{M^2 - v(\xi;m_K M Y d)}, \qquad (4.5)$$

where the deuteron mass is assumed to be small; g is the KNY coupling constant. For later use, we introduce $\mu(\xi;x)$,

$$\mu(\xi;x) = 2\pi\int_{-1}^{1} dz_v \frac{g\Gamma_0\,\rho(\xi;Mm_K)}{M^2 - v(\xi;m_K M\sqrt{x}\,d)}, \qquad (4.6)$$

so that

$$\mu(\xi;x=Y^2) = \frac{1}{\pi}\,\mathrm{Im}\,\Gamma_Y(\xi). \qquad (4.7)$$

We turn our attention to a consideration of the analyticity properties of the $dY\xi$ vertex. Define $\zeta(\xi,d^2)$ by the relation

$$\zeta(\xi,d^2) = \frac{2Q_0(\xi;Mm_K)Q_0(\xi;dY) - d^2}{2Q(\xi;Mm_K)Q(\xi;dY)}, \qquad (4.8)$$

where

$$Q_0(\xi;ab) = \frac{1}{2\sqrt{\xi}}\left[\xi + a^2 - b^2\right],$$

$$Q(\xi;ab) = \frac{1}{2\sqrt{\xi}}\left[\xi - (a+b)^2\right]^{1/2}\left[\xi - (a-b)^2\right]^{1/2}.$$

The z_v integral of Eq. (4.5) then becomes

$$\int_{-1}^{1} \frac{dz_v\, g\Gamma_0}{M^2 - \nu} = \int_{-1}^{1} \frac{dz_v\, g\Gamma_0}{2Q(\xi; M m_K) Q(\xi; dY)[\zeta(\xi, d^2) - z_v]} \quad . \tag{4.9}$$

The integral has singularities at $\zeta(\xi,d^2)=\pm 1$. For $d^2 < 4M^2$, the singularities are real with $\xi = 0$, $a_\pm$, and ∞, where

$$a_\pm = \frac{M^2+m_K^2 - Y^2}{2M^2} d^2 + Y^2 \pm M d \sqrt{\left(1 - d^2/4M^2\right)\left(1 - \left(\frac{Y-m_K}{M}\right)^2\right)\left(\left(\frac{Y+m_K}{M}\right)^2 - 1\right)} \, . \tag{4.10}$$

The z_v integral can now be transformed[71] into a contour integral in the ξ plane with cuts from $-\infty$ to 0 and from a_- to a_+. The result may be expressed in the form

$$\mathrm{Im}\,\Gamma_Y(\xi) = 2\pi^2 \rho(\xi; M m_K) \int d\xi' \frac{\mathrm{sign}\left(-\partial\zeta(\xi', d^2)/\partial\xi'\right)}{2Q(\xi'; M m_K) Q(\xi'; dY)(\xi' - \xi - i\varepsilon)} \quad , \tag{4.11}$$

where

$$\int = \int_{-\infty}^{0} + \int_{a_-}^{a_+} \quad .$$

Suppose the deuteron mass is small, say, smaller than Λ . It can be easily shown that a_+ increases with d^2 provided $d^2 < d_c^2 = 2M^2 - \frac{M}{m_K}(Y^2 - M^2 - m_K^2)$; $a_+ = (M+m_K)^2$ when $d^2 = d_c^2$, and then decreases as d^2 increases to its physical value. When the deuteron mass is sufficiently small, $\Gamma_Y(\xi)$ can be expressed in terms of $\mathrm{Im}\,\Gamma_Y(\xi)$ by means of the Cauchy theorem, viz.,

$$\Gamma_Y(\xi) = \frac{1}{\pi} \int_{(M+m_K)^2}^{\infty} d\xi' \frac{\mathrm{Im}\,\Gamma_Y(\xi')}{\xi' - \xi} \quad . \tag{4.12}$$

If, now, we add $-i\varepsilon(\varepsilon > 0)$ to d^2, a_+ will have a negative imaginary part when $d^2 < d_c^2$, and a positive imaginary part when $d^2 > d_c^2$. As d^2 increases to its physical value, a_+ approaches and goes around the normal threshold $(M+m_K)^2$, and then diminishes. Therefore, as d^2 increases, the singularity a_+ of Im $T_Y(\xi')$ cuts across the ξ' contour in Eq. (4.12), and a deformation of the ξ' contour becomes necessary in order to define $\Gamma_Y(\xi)$ for the physical deuteron mass.

To find a convenient expression for $\Gamma_Y(\xi)$, let us consider the general problem of analytic continuation with respect to d^2 of an integral,[71,72] $I(s,d^2)$, defined for small d^2 by

$$I(s,d^2) = \int_n^\infty \frac{ds'\, g(s')}{s'-s} \int_{-\infty}^{a(d^2)} \frac{ds''\, f(s'')}{s''-s'}, \tag{4.13}$$

where n and a are real and n > a. We assume here that

I. f(s) has a cut to the right of n;

II. g(s) is regular between $a(d^2_{\text{physical}})$ and n;

III. as d^2 increases, $a(d^2)$ varies as shown in Fig. 11 when d^2 has a small negative imaginary part;

and IV. $s \neq s'$.

In order that $I(s,d^2)$ remain on the same (physical) sheet as d^2 increases to its physical value, we have to deform the s' contour as shown in Fig. 11; $I(s,d^2)$ then becomes

$$I(s,d^2) = -2\pi i \int_a^n \frac{ds'\, f_{II}(s')\, g(s')}{s'-s} + \int_n^\infty \frac{ds'\, g(s')\, B(s')}{s'-s}, \tag{4.14}$$

where

$$B(s) = \int_{-\infty}^{a} \frac{ds' f(s')}{s'-s} + \int_{a}^{n} \frac{ds'}{s'-s}\left[f(s') - f_{II}(s')\right],$$

and $f_{II}(s)$ is the continuation of f(s) into the second sheet through the n cut from below. Equation (4.14) is the basis of the analytic continuation procedure which we shall use many times.

The result of the previous paragraph can now be applied to the study of the anomalous thresholds of the deuteron-hyperon vertex $\Gamma_Y(\xi)$ and of the double-scattering amplitude $T_d(u)$. We rewrite Eq. (4.12) in a somewhat more convenient form, viz.,

$$\Gamma_Y(\xi) = 2\pi g \Gamma_0 \int_{(M+m_K)^2}^{\infty} \frac{d\xi' \rho(\xi';Mm_K)}{\xi'-\xi} \left(\int_{-\infty}^{0} + \int_{a}^{a_+}\right) \frac{d\xi'' \,\mathrm{Sign}(-\partial\zeta(\xi',d^2)/\partial\xi'')}{2Q(\xi'';Mm_K)Q(\xi'';dY)(\xi''-\xi')}$$

The integrand of the ξ'' integral has two cuts in the ξ'' plane; these run from $(M-m_K)^2$ to $(d-Y)^2$ and from $(M+m_K)^2$ to $(d+Y)^2$, respectively.* As the deuteron mass d increase, a_+ increases, goes around $(M+m_K)^2$, and then decreases. Along with this process, the integrand has to be evaluated on the second sheet of the ξ'' plane through the cut from $(M+m_K)^2$ to $(d+Y)^2$. We can then immediately apply the results of the analytic continuation (Eqs. (4.13) and (4.14)) to $\Gamma_Y(\xi)$ and obtain, after a straightforward calculation,

$$\Gamma_Y(\xi) = \frac{1}{\pi}\int_{a_+}^{(M+m_K)^2} d\xi' \frac{\Im m_A \Gamma_Y(\xi')}{\xi'-\xi} + \frac{1}{\pi}\int_{(M+m_K)^2}^{\infty} d\xi' \frac{\Im m_N \Gamma_Y(\xi')}{\xi'-\xi}, \qquad (4.15)$$

---

* We note that $Q(\xi'';Mm_K)Q(\xi'';dY)$ includes the factor

$$\left\{\left[\xi''-(M+m_K)^2\right]\left[\xi''-(M-m_K)^2\right]\left[\xi''-(d+Y)^2\right]\left[\xi''-(d-Y)^2\right]\right\}^{1/2}.$$

where

$$\mathrm{Im}_A\,\Gamma_Y(\xi) = \frac{g\Gamma_0\,\theta(\xi - a_+)\,\theta((M+m_K)^2 - \xi)}{8\,\{[(d+Y)^2 - \xi][\xi - (d-Y)^2]\}^{1/2}}\ .$$

The values of a_+ turn out to be

$$a_+ = 33.9\mu^2, \qquad (d\Lambda\xi),$$
$$= 46.6\mu^2, \qquad (d\Sigma\xi).$$

For comparison, the normal threshold is given by

$$(M+m_K)^2 = 104.9\mu^2\ .$$

The integrand of the ξ'integral over the normal region ($(M+m_K)^2$ to ∞), $\mathrm{Im}_N\Gamma_Y(\xi)$, is obtained by a direct integration of the right-hand side of Eq. (4.5),

$$\mathrm{Im}_N\,\Gamma_Y(\xi) = \frac{g\Gamma_0\,\theta(\xi - (M+m_K)^2)}{16\pi i\{[(d+Y)^2 - \xi][\xi - (d-Y)^2]\}^{1/2}}\,\log\frac{\phi(\xi) + \sqrt{\psi(\xi)}}{\phi(\xi) - \sqrt{\psi(\xi)}}\ ,$$

where

$$\psi(\xi) = \frac{1}{4\xi^2}[\xi - (d+Y)^2][\xi - (d-Y)^2][\xi - (M+m_K)^2][\xi - (M-m_K)^2],$$

and

$$\phi(\xi) = \frac{1}{2\xi}[\xi^2 - (d^2 + Y^2 - M^2 - m_K^2)\xi + (d^2 - Y^2)(M^2 - m_K^2)]\ .$$

Now, it can be verified that $\mathrm{Im}\Gamma_Y(\xi)$ is a monotonically decreasing function of ξ; also, that it decreases faster with respect to increasing ξ in the normal region ($\xi \geq (M+m_K)^2$) than in the anomalous region ($a_+ \leq \xi \leq (M+m_K)^2$).

Therefore, we adopt the approximation that, in Eq. (4.15), the second integral (over the normal region) can be ignored compared to the first integral (over the anomalous region). Although it is possible to include the contribution from the second integral in the calculation of the double-scattering amplitude, our approximation greatly simplifies the problem.

We apply next the technique of analytic continuation to the double-scattering amplitude. Let us rewrite Eq. (4.4b) in terms of $\mu(\xi;x)$ (Eq. (4.7)):

$$\mathrm{Im}\, T_d(u) = -2\pi^2 \int_{(M+m_K)^2}^{(\sqrt{u}-M)^2} d\xi \left[G(u_-,\xi_-) + \tilde{G}(u_-,\xi_-)\right] \rho(u;M\sqrt{\xi})$$

$$\times \int_{-1}^{1} dz_x \frac{g\,\mu(\xi;x)}{Y^2 - x(u;M\sqrt{\xi}\,m_K d)}$$

$$= -2\pi^2 \int_{(M+m_K)^2}^{(\sqrt{u}-M)^2} d\xi \left[G(u_-,\xi_-) + \tilde{G}(u_-,\xi_-)\right] \rho(u;M\sqrt{\xi})\,\mu(\xi;Y^2)$$

$$\times \int_{-\infty}^{a_1} du' \frac{g}{2Q(u';M\sqrt{\xi})Q(u';m_K d)(u'-u-i\varepsilon)}\,, \qquad (4.16)$$

where the u' integral is obtained from the z_x integral in exactly the same way that we made the transition from (4.9) to (4.11), and $u' = a_1$ is defined as the end-point singularity of the u' integral.

We consider the ξ integral. If in the expression for $\mu(\xi;Y^2)$ the deuteron mass increases, one of the singularities of $\mu(\xi;Y^2)$ cuts across the ξ contour, and we encounter again the need for carrying out an analytic continuation. The procedure is very similar to the case of Eq. (4.12), and Im $T_d(u)$ becomes, retaining only $\mathrm{Im}_A \Gamma_Y(\xi)$,

$$\mathrm{Im}\, T_d(u) = -2\pi \int_{a_+}^{(M+m_K)^2} d\xi \left[G(u_-,\xi_-) + \tilde{G}(u_-,\xi_-)\right] \rho(u;M\sqrt{\xi})\, \mathrm{Im}_A \Gamma_Y(\xi)$$

$$\times \int_{-\infty}^{a_1} du' \frac{g}{2Q(u';M\sqrt{\xi})Q(u';m_K d)(u'-u)}\,, \qquad (4.17)$$

where a_+ was defined in Eq. (4.10). Let

$$H(u) = \int_{-\infty}^{a_1} du' \frac{g}{2Q(u';M\sqrt{\xi})Q(u';m_K d)(u'-u)} ;$$

$T_d(u)$ can then be expressed as

$$T_d(u) = -2\int_{a_+}^{(M+m_K)^2} d\xi \int_{(M+\sqrt{\xi})^2}^{\infty} \frac{du'}{u'-u}\left[G(u'_-,\xi_-) + \tilde{G}(u'_-,\xi_-)\right]$$

$$\times \rho(u';\sqrt{\xi}M)\, \mathrm{Im}_\Lambda \Gamma_Y(\xi)\, H(u'). \qquad (4.18)$$

Now, the u'-integral contour of Eq. (4.18) may have to be modified due to the singularities of $G(u',\xi)$ and $H(u')$ as the deuteron mass increases. It is easily shown, however, from simple geometry that the singularity a_1 of $H(u')$ will never reach the normal threshold of the u' integral, $(M+\sqrt{\xi})^2$, for any ξ. On the other hand, $G(u',\xi)$ will have a (real) singularity, a_2, in the u' plane* which appears in the physical u' sheet as d^2 increases for $\xi < \xi_0 = M + m_K - 2\,\delta(1+Mm_K^{-1})$ (δ is the binding energy of the physical deuteron). Therefore, a modification of the u' contour will be necessary. Finally, it can be shown that no additional singularities[73,74] will arise in $G(u',\xi)$ as ξ varies.

We obtain finally for the double-scattering amplitude $T_d(u)$,

$$T_d(u) = \frac{1}{\pi}\int_{u_0(a_+)}^{(2M+m_K)^2} du' \frac{\mathrm{Im}\, T_d(u')}{u'-u} , \qquad (4.19a)$$

---

*This may be most easily seen by taking $G(u',\xi)$ to be the S-wave projection of a one-nucleon-exchange approximation for the $K^+d \to KNN$ amplitude. One then has also $G(u',\xi) = \tilde{G}(u',\xi)$.

where

$$\operatorname{Im} T_d(u) = \frac{\pi g \Gamma_0}{8\{[u-(d-m_K)^2][(d+m_K)^2-u]\}^{1/2}} \int_{a_+}^{(M+m_K)^2} d\xi f(\xi)\theta(\xi_0-\xi)$$

$$\times\, \theta(u-u_0(\xi))\operatorname{Im}_\Lambda \Gamma_Y(\xi) \int_{-\infty}^{a_1} \frac{du'}{2Q(u';M\sqrt{\xi})Q(u';m_K d)(u'-u)}\,, \qquad (4.19b)$$

with $u_o(\xi) = a_2$, and $f(\xi)$, the KN → KN amplitude, is as shown in Fig. 12.

The method we have developed can be applied to derive the dispersion relation for the impulse approximation term $T_i(t)$ with the result

$$T_i(t) = \frac{\Gamma_0^{\,2}}{8\pi} \int_{t_0}^{4M^2} \frac{dt'\, g(t')}{(t'-t)\sqrt{t'(4d^2-t')}}\,, \qquad (4.20)$$

where $t_o = 1.73\mu^2$.

The anomalous threshold $u_o(a_+)$ of the double-scattering amplitude can be easily calculated. For $\bar{K}d$ scattering,

$$u_o(a_+) = 195.4\mu^2$$

if the hyperon (the propagator corresponding to x in Fig. 10b) is a Λ;

$$u_o(a_+) = 166.8\mu^2$$

if the hyperon is a Σ. These values are to be compared with the normal threshold, $(2M+m_K)^2 \approx 287\mu^2$. For the case of πd scattering, which can be handled in an analogous way, one has

$$u_o(a_+) \approx 4M^2,$$

which is very close to the normal threshold $(2M+\mu)^2 \approx 4M^2(1+0.15)$. Thus, for πd scattering, the effect of the double-scattering correction to the impulse approximation is expected to be very small. On the other hand, this correction will play a significant role in the case of $\bar{K}d$ scattering.

V. A SIMPLE MODEL--BOX DIAGRAMS

In the last section, we studied the analyticity properties of the triangle diagrams which correspond to πd and $\bar{K}d$ scattering. There, we noted that the existence of very small anomalous thresholds in the t or u channel is a main feature of the low-energy scattering amplitude and that this in turn makes the overall analysis easier. Although some of the elastic-scattering amplitudes can be approximated by simple triangle diagrams, as will be discussed in Sec. VII, in practice, we generally need to know the singularities of the amplitudes in the s channel as well.

We accordingly consider the analyticity properties of the scattering amplitudes in terms of generalized box diagrams. Toward this end, we shall define the corresponding impulse approximation, the binding corrections, and the multiple-scattering corrections. Once again we come back to Figs. 4a - 4c. As in the case of the triangle diagrams, the probability that a deuteron will break up into two nucleons ($d \to NN$) in the intermediate state of the s channel is assumed to be very large compared to other possibilities such as $d \to d\pi$, $d \to NN\pi$, etc. Therefore, the lower blobs of Figs. 4a - 4c can be regarded as propagators consisting of single nucleons. (The possibilities of Figs. 8b - 8d are then excluded.)

The impulse approximation is then the scattering amplitude corresponding to Fig. 8a. From Figs. 4b and c, we obtain the diagrams which correspond to the binding corrections (Figs. 13a and b) and the multiple (triple) scattering terms (Fig. 13c).* For the sake of definiteness, we shall consider πd scattering

*Here, the s' should be understood as propagators. We have not considered the the general case where the upper blobs of Fig. 4 are retained. The analyticity properties of such terms are more involved in general than the cases we shall be dealing with.

in this section. As noted at the end of the last section, double-scattering effects can be ignored.

We begin with the unitarity relation, Eq. (4.2), applied to the various amplitudes in the t channel. Consider, in particular, the binding-correction term, denoted by $T_b(t,s)$ (Fig. 13b). The imaginary part of the amplitude in the t channel assumes the following form, when t is above the normal threshold $(2M+\mu)^2$ and s is in the unphysical region (for the s channel process $\pi d \to \pi d$) and all internal propagators correspond to particles with definite masses:*

$$\mathrm{Im}\, T_b(t,s) = -\pi g^2 \gamma_0^2 \int d\xi\, f(\xi)\, \rho(t; \sqrt{\xi} M)\, \rho(\xi; M\mu)$$
$$\times \int_{-1}^{1} \frac{dz_x\, d\phi}{(s' - M'^2)(x - M_x^2)} \int_{-1}^{1} \frac{dz_v\, d\phi'}{v - M^2}, \qquad (5.1)$$

where we have used the same notation as in Sec. IV; the amplitude, of course, represents the $d\bar{d} \to \pi\pi$ process. We assume here again that the deuteron mass is so small that there is no anomalous threshold in the t channel. In Eq. (5.1), $f(\xi)$ is the πN scattering amplitude of Fig. 13b, which we assume to be a function of ξ only,** and not of ω (ω is the invariant momentum transfer for the πN scattering).

The ϕ' integral can be carried out, with the result,

---

*For the sake of generality, we denote the masses associated with the s' and x propagator by M' and M_x, respectively.

**This assumption, which is reasonable so long as we are dealing with low-energy reactions, is essential in the reduction of diagrams with three-body intermediate states to those with two-body states.

$$\mathrm{Im}\, T_b(t,s) = \frac{1}{32\pi^2\sqrt{t}} \int d\xi f(\xi)\mu(\xi; M_x^2) Q(t;\sqrt{\xi},M) \int d\Omega\, T_2^* T_1 \,, \tag{5.2}$$

where $\mu(\xi;M_x^2)$ is given by Eq. (4.6), $T_1 = \frac{\Gamma_o}{x-M_x^2}$ is the amplitude from the initial state ($d\bar{d}$) to the intermediate state ($\bar{\xi}N$), and $T_2 = \frac{g}{s'-M'^2}$ refers to the amplitude from the final state ($\pi\pi$) to the intermediate state. The quantity Q is defined in (2.14) and $d\Omega = dz_x\, d\phi$. As we saw in detail in Sec. IV, the integration limits of the ξ integral may be taken from a_+ to $(M+\mu)^2$, where a_+ is the anomalous threshold of the deuteron-nucleon ($dx\xi$) vertex.

Equation (5.2) shows that Im $T_b(t,s)$ in the t channel can be expressed in terms of the amplitude for the simple box diagram shown in Fig. 13b'; as in the case of the triangle diagrams, here too the deuteron-nucleon vertex, $\mu(\xi;M_x^2)$, will play an important role in the study of the analyticity of the πd scattering amplitude. [One can also write down, in a similar manner, the imaginary part of the triple-scattering amplitude (Fig. 13c); it will be characterized by two deuteron-nucleon vertices (Fig. 13c').]

Consider that part of the right-hand side of Eq. (5.2) which has exactly the same form as the imaginary part of the scattering amplitude with two-body intermediate states; thus, we introduce T_ξ, where

$$\mathrm{Im}\, T_\xi = -\frac{Q(t;\sqrt{\xi}M)}{32\pi^2\sqrt{t}} \int d\Omega\, T_2^* T_1 \,. \tag{5.3}$$

Let z, z_1, and z_2 be the cosines of the angles between the three-momenta of the initial d and an outgoing π, the initial d and the intermediate N, and the intermediate N and the π, respectively. Eq. (5.3) then becomes

$$\mathrm{Im}\, T_\xi = -\frac{Q(t;\sqrt{\xi}M)}{32\pi^2\sqrt{t}} \int_{-1}^{1} \frac{dz_1}{2Q(t;dd)Q(t;\sqrt{\xi}M)(z_1-\zeta_1)} \int_{z_2^-}^{z_2^+} \frac{dz_2}{2Q(t;\sqrt{\xi}M)Q(t;\mu\mu)(z_2-\zeta_2)\sqrt{K(z,z_1,z_2)}} \,, \tag{5.4}$$

where $$K(z, z_1, z_2) \equiv 1 - z^2 - z_1^2 - z_2^2 + 2 z z_1 z_2$$
and $$z_2^{\pm} = z z_1 \pm \sqrt{1-z^2}\sqrt{1-z_1^2} \quad ;$$

also (see Eq. (4.8)),
$$\zeta_1 = \left(2Q_0(t; dd)Q(t; M\sqrt{\xi}) - M_x^2\right) \Big/ \left(2Q(t; dd)Q(t; M\sqrt{\xi})\right),$$

$$\zeta_2 = \left(2Q_0(t; \mu\mu)Q_0(t; M\sqrt{\xi}) - M'^2\right) \Big/ \left(2Q(t; \mu\mu)Q(t; M\sqrt{\xi})\right).$$

The z_1 integral can be transformed in the t plane into a contour integral from $-\infty$ to t_0 (cf. Eq. (4.11)), where t_0 corresponds to $\zeta_1 = \pm 1$ and is given by

$$t_0 - t_0(\xi) = \frac{d^2}{2M^2}(3M^2 + \xi - d^2) + \frac{d}{2M^2}\sqrt{(4M^2 - d^2)((\sqrt{\xi}+M)^2 - d^2)(d^2 - (\sqrt{\xi}-M)^2)} \,. \quad (5.5)$$

We have used the fact that the z_2 integral is analytic for $-1 \leq z_1 \leq 1$. For fixed ξ and a small deuteron mass, T_ξ can be expressed in the form of a dispersion relation in the t plane. As the deuteron mass increases to its physical value, t_0 goes around the normal threshold $(\sqrt{\xi}+M)^2$, so that one needs to modify the contour in the t plane. Retaining only the anomalous region $t_0 \leq t \leq (\sqrt{\xi}+M)^2$, we obtain for T_ξ, for the physical deuteron mass,

$$T_\xi = \frac{1}{16\pi^2}\int_{t_0}^{(\sqrt{\xi}+M)^2} \frac{dt'}{(t'-t)\sqrt{t'(4d^2-t')}} \left[\frac{A(z,\zeta_1)}{2Q(t'; M\sqrt{\xi})Q(t'; \mu\mu)}\right], \quad (5.6)$$

where

$$A(z, \zeta_1) = \int_{z_2^-}^{z_2^+} \frac{dz_2}{(z_2 - \zeta_2)\sqrt{K(z, \zeta_1, z_2)}} \,. \quad (5.7)$$

The complete dispersion relation for $T_b(t,s)$ for a real deuteron with s unphysical (with respect to the s channel) is, from Eqs. (5.2) and (5.6),

$$T_b(t, s) = -\frac{1}{16\pi^2}\int_{a_+}^{(M+\mu)^2} d\xi\, f(\xi)\mu(\xi; M_x^2) \int_{t_0(\xi)}^{(\sqrt{\xi}+M)^2} \frac{dt'}{(t'-t)\sqrt{t'(4d^2-t')}}$$
$$\times \int_{s'_-}^{s'_+} \frac{ds'}{(s'-M'^2)\sqrt{(s'_+-s')(s'-s'_-)}} \,, \quad (5.8)$$

where

$$s_{\pm}' = \mu^2 + M^2 - 2Q_0(t'; M\sqrt{\xi})Q_0(t'; \mu\mu) + 2Q(t'; M\sqrt{\xi})Q(t'; \mu\mu)z_2'^{\pm}$$

and

$$z_2'^{\pm} = z\zeta_1 \pm \sqrt{(1-z^2)(1-\zeta_1^2)}\,.$$

In the application of Eq. (5.8) to the πd scattering problem, it is still necessary to continue it analytically into the physical region of s. In the course of this analytic continuation in s, the singularities of the s' integral in the t' plane may cut across the t' contour (t_0 to $(M+\sqrt{\xi})^2$). In this event, we will need to modify the t' contour. Therefore, we seek to determine the details of the singularity of T_ξ as a function of s, which is, of course, equivalent to finding the Landau curve of T_ξ as defined in Eq. (3.3a).

The Landau curve may be obtained by solving (3.3a) for t as a function of s, or, equivalently, the equation, $z_a^2+z_b^2+z_c^2-2z_az_bz_c-1 = 0$, with the intermediate particles in the s and t channels on the mass shell, and where z_a, z_b, z_c are the cosines of the scattering angles as shown in Fig. 13b'. A straightforward calculation gives for the case of Fig. 13b' the following result:

$$\begin{aligned} t = t_{\pm}(s,\xi) = &-\frac{1}{2s}\left[s-(d+\mu)^2\right]\left[s-(d-\mu)^2\right] \\ &+\frac{1}{2Q^2(s; M'M_x)}\left\{M^2+\frac{1}{2s}\left[s^2-(\mu^2+d^2+M'^2+M_x^2)s+(d^2-\mu^2)(M_x^2-M'^2)\right]\right\} \\ &\times\left\{\xi+\frac{1}{2s}\left[s^2-(\mu^2+d^2+M'^2+M_x^2)s+(d^2-\mu^2)(M_x^2-M'^2)\right]\right\} \\ &\pm\frac{M\sqrt{\xi}}{2s\,Q^2(s; M'M_x)}\left[(s-s_+^e)(s-s_-^e)(s-s_+^o)(s-s_-^o)\right]^{1/2}, \end{aligned} \qquad (5.9)$$

and $s_{\pm}^e$ and $s_{\pm}^o$ are the s corresponding to $z_a = \pm 1$, and $z_b = \pm 1$, respectively, calculated on the mass shell.

In Eq. (5.9), the $s_{\pm}^{o}$ are the anomalous thresholds of the πd scattering amplitude in the s channel (in the physical or unphysical sheet) for the reaction $\pi d \to M' M_x$ with ξ exchange, and $s_{\pm}^{e}$ are the corresponding anomalous thresholds for $\pi d \to M' M_x$ with N exchange. In particular, if $M' = M_x = M$, the Landau curve and the $s_{\pm}^{e(o)}$ assume the following simpler forms:

$$t = t_{\pm}(s, \xi) = -\frac{1}{2s}\left[s-(d+\mu)^2\right]\left[s-(d-\mu)^2\right] + \frac{1}{4Q^2}\left[s-(d^2+\mu^2)\right]\left[\xi - M^2 + (s-d^2-\mu^2)/2\right]$$

$$\pm \frac{M\sqrt{\xi}}{2sQ^2}\left[(s-s_+^e)(s-s_-^e)(s-s_+^o)(s-s_-^o)\right]^{1/2} \tag{5.10}$$

where

$$Q = Q(s; MM) = \sqrt{s-4M^2}/2 \; ,$$

$$s_{\pm}^{e} = d^2+\mu^2 - \frac{\mu^2 d^2}{2M^2} \pm 2d\mu\sqrt{(1-d^2/4M^2)(1-\mu^2/4M^2)} \; ,$$

and

$$s_{\pm}^{o} = 2M^2 + \frac{1}{2\xi}(\xi + M^2 - \mu^2)(d^2 - \xi - M^2)$$

$$\pm \frac{1}{2\xi}\left\{\left[(d+M)^2-\xi\right]\left[\xi-(d-M)^2\right]\left[(M+\mu)^2-\xi\right]\left[\xi-(M-\mu)^2\right]\right\}^{1/2} . \tag{5.11}$$

When the two exchanged particles N and ξ are the same, $s_{\pm}^{e} = s_{\pm}^{o}$. If $M' = M_x = M = \sqrt{\xi}$, which corresponds to a simple box diagram for elastic πd scattering (Fig. 5a with all intermediate masses equal), then

$$t_+(s) = \frac{4M^2(s-s_+^e)(s-s_-^e)}{s(s-4M^2)} \; ,$$

and

$$t_-(s) = 0 \; ,$$

results which were already obtained in Eq. (3.35). In the present instance, the $s_{\pm}^{e}$ and $s_{\pm}^{o}$ are generally different, and the Landau curve will be more complicated. A typical curve $t = t_+(s,\xi)$ (Eq. 5.10) for a given ξ is shown in Fig. 14. The threshold $t_0(\xi)$ decreases as ξ decreases, and assumes its minimum value $t_0 = 11\mu^2$ when $\xi = a_+$ (Eq.(4.10)); this is just the anomalous threshold in the t channel of the binding-correction term, as shown in Figs. 9a and a'.

We are finally in a position to continue analytically our dispersion relation (5.8) into the physical region of s. For this purpose, we first express this relation in a somewhat different form. It is not difficult to prove the equality,

$$t(4d^2-t)(s_+'-M^2)(M^2-s_-') = s(4M^2-s)(t_+(s,\xi)-t)(t-t_-(s,\xi)),$$

for the case that $M' = M_x = M$ in Fig. 13b'. The s'-integral in Eq. (5.8) can be carried out, giving the result $2\pi i \dfrac{1}{\sqrt{(s_+'-M^2)(M^2-s_-')}}$.

The t' integral then becomes

$$2\pi i \int_{t_0(\xi)}^{(\sqrt{\xi}+M)^2} \frac{dt'}{(t'-t)\sqrt{s(4M^2-s)(t_+(s,\xi)-t')(t'-t_-(s,\xi))}} .$$

This integral is defined when s is in an unphysical region of the s channel, say, s is positive and very small. As s increases, the singularities of the integrand $t' = t_\pm(s)$ move in the t' plane. If they cut across the t' contour, the contour will need to be modified so as to avoid these singularities. Referring to Fig. 14, we see that this may happen when $s = s_+^e$, and when $s = s_m$ (which corresponds to the anomalous threshold $t_0(\xi)$). Adding $+i\varepsilon$ to s, we find that near $s = s_+^e$ the singularities $t' = t_\pm(s)$ move as shown in Fig. 15. Therefore, as s passes s_+^e, the t' integral remains the same. On the other hand, near $s = s_m$, $t' = t_+(s)$ varies as shown in Fig. 16, and the t'-integral contour must be modified accordingly. The other singularity $t' = t_-(s)$ will not reach the t' contour for $s > s_+^e$.

The dispersion relation (5.8) can now be continued into the physical region of s; the final result becomes

$$T_b(t,s) = -\frac{g\Gamma_0}{16\pi}\int_{a_+}^{(M+\mu)^2} d\xi\, f(\xi)\mu(\xi;M^2)\Big[\int_{t_0(\xi)}^{t_+(s,\xi)} \frac{dt'}{(t'-t)\sqrt{s(s-4M^2)(t_+(s,\xi)-t')(t'-t_-(s,\xi))}}$$

$$- i\int_{t_+(s,\xi)}^{(\sqrt{\xi}+M)^2} \frac{dt'}{(t'-t)\sqrt{s(s-4M^2)(t'-t_+(s,\xi))(t'-t_-(s,\xi))}}\Big]. \qquad (5.12)$$

In the case of the box diagram (Fig. 8a) for the impulse approximation, the πd scattering amplitude can be expressed in a form similar to Eq. (5.12). In particular, corresponding to Fig. 8a (with s' replaced by a single nucleon), the dispersion relation for the scattering amplitude, denoted by $T_{i1}(t,s)$, for fixed s in the physical region of the s channel takes on the following form:[30]

$$T_{i1}(t,s) = \frac{g^2\Gamma_0^2}{16\pi}\Big[\int_{t_0}^{t(s)} \frac{dt'}{(t'-t)\sqrt{s(s-4M^2)t'(t(s)-t')}}$$

$$- i\int_{t(s)}^{4M^2} \frac{dt'}{(t'-t)\sqrt{s(s-4M^2)t'(t'-t(s))}}\Big], \qquad (5.13)$$

where $t = t(s)$ is the Landau curve (see (3.5)) for the box diagram, and t_o is the anomalous threshold for this diagram in the t channel and is given by $t_o = 1.73\mu^2$ (Eq. (3.4). Corresponding to $t = t_-(s)$ (the other branch of the Landau curve) in Eq. (5.12), we have, in the present instance, simply $t = 0$ (see Eq. (3.5)). Equation (5.12) will be applied in the calculation of the binding-correction terms to the impulse approximation in Sec. VI. The present technique can also be applied to more complicated problems, e.g., the multiple-scattering correction; here, however, a detailed calculation is not essential (we will return to this point in the next section).

VI. THE ELASTIC SCATTERING OF π^+ MESONS BY DEUTERONS

We now apply the dispersion relations (5.12) and (5.13) to the πd and $\bar{K}d$ scattering problems. In Eqs. (5.12) and (5.13) the scattering amplitudes for given s are expressed in the form of integrals over t' (the momentum-transfer variable). Thus the immediate application of our dispersion relations is in the calculation of angular distributions at fixed energy.

In Sec. V we defined the impulse approximation in terms of box diagrams, viz., it is the amplitude $T_i(t,s)$ corresponding to Fig. 8a. The corresponding dispersion relations (similar to Eq. (5.13)) have been studied extensively by Brehm and Sucher.[30] These authors have represented the πN scattering amplitude in terms of simple T matrices of the type $\frac{C_1}{s-M_1^2}$, $\frac{C_2}{t-M_2^2}$, $\frac{C_3}{u-M_3^2}$, and a constant D, where the C_i's are essentially coupling constants and D is determined so as to reproduce the low-energy πN scattering. Among these T-matrices, the important contribution to the impulse approximation comes from two such terms, one of which corresponds to the p-wave (3,3) resonance ($N^*_{3/2}$), also approximated by a simple T matrix, and the other corresponds to a single-nucleon propagator.

In this section, we consider the binding corrections and the multiple (triple) scattering* terms defined in Sec. V (see Fig. 13), and determine the effect of these terms on the angular distribution of elastic πd scattering.

Take first the binding-correction terms which are shown, for the case of $\pi^+ d$ scattering, in Fig. 17. The circled part of each diagram corresponds to the $f(\xi)$ defined in Eq. (5.1). The propagators denoted by s' in

---

*The double-scattering term may be neglected (see the discussion at the end of Sec. IV).

Figs. 17a - d represent single-nucleon propagators of the type $\frac{1}{s'-M^2}$. The propagators denoted by N^* correspond to the $N^*_{3/2}$ particle. There are other diagrams representing binding corrections, but for the purpose of comparing a binding correction with its corresponding impulse-approximation form, we study only those diagrams which are shown in Fig. 17. We determine first the scattering amplitudes for Figs.17a and 17b (denote the sum by T_{b1}) and then take up the other diagrams, Figs. 17c and 17d (denoted by T_{b2}).

Introduce I_1 and I_2 to represent the two terms of the t' integral of (5.12), viz.,

$$I_1 = \int_{t_0(\xi)}^{t_+(\Delta,\xi)} \frac{dt'}{(t'-t)\sqrt{\Delta(\Delta-4M^2)(t_+(\Delta,\xi)-t')(t'-t_-(\Delta,\xi))}},$$

and

$$I_2 = -i\int_{t_+(\Delta,\xi)}^{(\sqrt{\xi}+M)^2} \frac{dt'}{(t'-t)\sqrt{\Delta(\Delta-4M^2)(t'-t_+(\Delta,\xi))(t'-t_-(\Delta,\xi))}},$$

where $t_0(\xi)$ is the anomalous threshold, and $t = t_+(s,\xi)$ is the Landau curve (Eq. 5.10). Upon carrying out the t' integrations, we obtain, for I_1 and I_2,

$$I_1 = \frac{1}{\sqrt{(t_+(\Delta,\xi)-t)(t_-(\Delta,\xi)-t)}}\left\{\frac{\pi}{2} - \sin^{-1}\left[1+2\frac{(t_0(\xi)-t_+(\Delta,\xi))(t_-(\Delta,\xi)-t)}{(t_0(\xi)-t)(t_+(\Delta,\xi)-t_-(\Delta,\xi))}\right]\right\},$$

$$I_2 = \frac{i}{\sqrt{(t_+(\Delta,\xi)-t)(t_-(\Delta,\xi)-t)}}\log\left\{1+2\frac{(t_-(\Delta,\xi)-t)(b-t_+(\Delta,\xi))-\sqrt{A}}{(b-t)(t_+(\Delta,\xi)-t_-(\Delta,\xi))}\right\}, \tag{6.1}$$

where

$$A = (t_+(\Delta,\xi)-t)(t_-(\Delta,\xi)-t)(b-t_-(\Delta,\xi))(b-t_+(\Delta,\xi)),$$

$$b = (\sqrt{\xi}+M)^2.$$

At this stage, we need to consider briefly several miscellaneous points. Since we are dealing with scalar particles, the (charge-symmetric) pion-nucleon coupling constant g cannot be identified with the usual (ps-pv) renormalized coupling constant $f^2 = 0.082$;[75] to compare g and f, we express the π^+p scattering amplitude (for example) in two ways (with spins and without), with the result $g^2 = 380\mu^2$.*

Corresponding to the N^* propagator, we define g_{33} as the (scalar) $N^*N\pi$ coupling constant. The value of g_{33} as well as that of the dNN coupling constant Γ_o are those used by Brehm and Sucher,[30] viz.,

$$g_{33}^2 = 990\mu^2 \qquad \text{and} \qquad \Gamma_o^2 = 1470\mu^2 .$$

For the diagrams 17a and b, $f(\xi)$ takes the form $\frac{g^2}{s''-M^2}$ which we approximate by $\frac{g^2}{\mu(2M+\mu)}$, assuming $s'' \approx (M+\mu)^2$. The deuteron-nucleon vertex $\mu(\xi;M^2)$ has already been defined (Eq. (4.6)) and is

$$\mu(\xi;M^2) = \frac{1}{8\pi}\frac{1}{\sqrt{(d+M)^2-\xi}\sqrt{\xi-(d-M)^2}}$$

in the range of ξ entering in Eq. (5.12).

We can now calculate T_{b1}, where we make use of Eqs. (5.12) and (6.1). In order to compare the result with experiment, we express T(t,s) in terms of the non-invariant scattering amplitude f(t,s) defined in Eq. (2.11). Numerical calculations have been carried out with the aid of the Brown University IBM 7070 computer. The angular dependence at 85 MeV of the π^+d scattering amplitude f(t,s) is given in Table I, with and without[30]

*For the derivation of this result, see Sec. 18.10 of Ref. 64; see also Ref. 30.

the binding corrections. In Table I, f_i, the impulse approximation, is the sum of the three terms, f_{i1}(Fig. 8a with $s' \to N$), f_{i2} ($s' \to N^*_{3/2}$), and f_{i3} ($s' \to$ the other possible interactions[30]). Corresponding to the binding-correction terms T_{b1} (Figs. 17a and b) and T_{b2} (Figs. 17c and d), we introduce f_{b1} and f_{b2}. The angular distribution of the π^+d scattering cross section is shown in Fig. 18 in the laboratory system.

We see from Table I that f_{b1} is about 10% of f_{i1} over all angles, and is destructive relative to f_{i1}. However, since the total impulse term f_i is dominated[30] by f_{i2}, f_{b1} changes the differential cross section by only a few percent and leads to an almost constant increase over all angles as may be seen from Fig. 18. For comparison, the angular distribution calculated by Rockmore[16] in his phenomenological treatment is also given; this is in very good agreement with experiment.[15]

The total cross section (σ_{tot}) calculated from the optical theorem, $\sigma_{tot} = \frac{4\pi}{q}\,\mathrm{Im}\, f(t=0,s)$ (where q is the center-of-mass momentum of the incident pion), yields 25.4mb (in the impulse approximation[30]), 24.5mb (with binding corrections of the type f_{b1}), while the experimental value[15] is 37.7mb.

In view of the importance of $N^*_{3/2}$ in low-energy πN scattering, we have also determined the binding corrections (f_{b2}) given by Figs. 17c and d. The πN scattering is predominantly p wave near the energy corresponding to the $N^*_{3/2}$ state. We therefore assume that $f(\xi)$ in T_{b2} (see Eq. (5.12)) has the form, $\frac{g_{33}^2 \cos\theta}{s'' - M^{*2}}$, where θ is the scattering angle in the s'' channel. We take the mass M^* of the $N^*_{3/2}$ state to be 8.88 μ, neglecting the width of the state relative to M^*.

Approximating s" and cos θ by the expressions,

$$s'' = M^2 + \mu^2 - \frac{\xi^2 - (M^2 - \mu^2)^2}{2\xi},$$

$$\cos\theta = 1 + \frac{2\xi M^{*2}}{[M^{*2} - (M+\mu)^2][M^{*2} - (M-\mu)^2]},$$

we find that the resultant f_{b2} is about 10 times larger than f_{b1} and negative relative to it. The angular distributions of the scattering amplitude $f_i + f_{b2}$ together with the corresponding differential cross section are given in Table II and Fig. 18, respectively. The essential result is that there is a substantial decrease in the differential scattering cross section over all angles. The total cross section, obtained from the optical theorem, equals 35 mb.

While the significant binding corrections, those denoted by f_{b2}, do effect an improvement on the impulse approximation, one still needs some form of correction term which is large in the backward direction. We have estimated the order of magnitude of the triple-scattering diagram (Fig. 13c), but have found that even if we insert an $N^*_{3/2}$ into the circled parts of the diagram, the corrections to the impulse approximation are too small.

The absorption amplitude (Fig. 4e) is the only one whose forward-backward ratio[30] is less than unity, but both this amplitude, as well as its (double-scattering) correction term, are negligible. The main correction to the impulse approximation then seems to come from the $N^*_{3/2}$ binding term.

Several comments relative to the details of the calculation are in order at this point. First, the correction terms to the impulse approximation which we have determined depend very much on the choice of $f(\xi)$, the πN scattering amplitude in the ξ channel. We have assumed that the amplitude is a function of ξ only, and not of the angular variable. In the region of ξ we have considered (below the normal threshold of the πN scattering), this assumption appears not unreasonable (certainly at the normal threshold it is correct).

Second, although we have calculated the individual binding corrections f_{b1} and f_{b2} in order to determine which correction is more important, the $f(\xi)$ should have been a linear combination of a term with I(isotopic spin) = 1/2 and one with I = 3/2 according to the requirements of crossing symmetry (the substitution law).[32] In point of fact, because of the dominance of the interaction in the $N^*_{3/2}(I = 3/2)$ state, the essential conclusions of our calculation remain unchanged.

Lastly, we note that, within the framework of a dispersion-theoretic formulation of the πd problem with spinless particles, we have obtained about as reasonable an agreement with experiment as can be expected.

One could also try to take into account the contribution of the normal region to the scattering amplitude. However, this extension goes beyond the scope of the formalism developed in this paper.

VII. THE ELASTIC SCATTERING OF K^- MESONS BY DEUTERONS

As a second application of the analytic-continuation procedure which was developed in Secs. IV and V, we consider in this section the problem of K^-d elastic scattering. First, we shall define the impulse approximation for this case, and then proceed to calculate the angular distribution for the scattering at* $k = 105$ MeV/c and 300 MeV/c (k is the K^--meson laboratory momentum). Our results will then be compared with those of Hetherington and Schick.[29]

The low-energy $\bar{K}N$ reactions occur predominantly in s states and may be represented[76,77] by two complex scattering lengths, A_0 and A_1, where the subscripts refer to the isotopic-spin states of the $\bar{K}N$ system. The fact that there is a complex scattering length for each isotopic-spin state suggests that a single propagator with a complex mass (a resonance or a bound state) for each state may be used to reproduce the K^-N scattering. If this is the case, the impulse approximation is easily set up. We now investigate this possibility.

Consider the following elastic scattering processes at low energy:

$$\begin{aligned} K^-p &\longrightarrow K^-p \ , \\ K^-n &\longrightarrow K^-n \ . \end{aligned} \tag{7.1}$$

We assume that the scattering amplitudes for these processes can be expressed in terms of two propagators (depending on the isotopic spin) with masses Y_0 and Y_1, and with widths Γ_0 and Γ_1, respectively. This will be referred

---

*Corresponding to laboratory energies of 11 and 84 MeV, respectively.

to as the two-complex-pole approximation. The $\bar{K}N$ scattering amplitudes then become

$$f(I=0) = -\frac{1}{8\pi\sqrt{s}} \frac{g^2}{s-(Y_0^2 - i\Gamma_0)}$$
$$f(I=1) = -\frac{1}{8\pi\sqrt{s}} \frac{g^2}{s-(Y_1^2 - i\Gamma_1)} \tag{7.2}$$

In order to determine the masses and widths, we let these amplitudes approach the known scattering lengths at zero kinetic energy which we take to be the Humphrey-Ross[78] solutions. These are:

Solution I,

$$A_0 = -0.22 + 2.74i, \qquad A_1 = 0.02 + 0.38i;$$

Solution II, (7.3)

$$A_0 = -0.59 + 0.96i, \qquad A_1 = 1.20 + 0.56i,$$

where all lengths are expressed in fermis (10^{-13}cm).

Upon comparing Eqs. (7.2) and (7.3) we obtain the following results:

Solution I,

$$I=0, \qquad Y_0 = 10.25\mu, \quad \Gamma_0' = 11.2 \text{ MeV},$$
$$I=1, \qquad Y_1 = 10.27\mu, \quad \Gamma_1' = 84 \text{ MeV}; \tag{7.4}$$

Solution II,

$$I=0, \qquad Y_0 = 10.19\mu, \quad \Gamma_0' = 28.8 \text{ MeV},$$
$$I=1, \qquad Y_1 = 10.32\mu, \quad \Gamma_1' = 9.5 \text{ MeV}, \tag{7.5}$$

where $\Gamma_0' = \Gamma_0/Y_0$ and $\Gamma_1' = \Gamma_1/Y_1$.

In the determination of the above masses and widths, we have assumed that the magnitude of the coupling constant g^2 is $400\mu^2$. Also, we note that we have not attempted to include the effects of reactions in the crossed channels on the scattering amplitudes in the direct channel, since the crossed-channel reactions are not well known quantitatively. We will return to this point later.

We need next to check whether the two-complex-pole approximation really represents the actual behavior of $\bar{K}N$ scattering. Accordingly, the total cross section for K^-p elastic scattering from k = 50 MeV/c to 250 MeV/c was calculated for each type of solution. The results are shown in Fig. 19. It is evident that, between 100 and 250 MeV/c, both types of solution give reasonable agreement with experiment.[79]

We now define the scattering amplitude in the impulse approximation as that corresponding to Fig. 5a in which $s' \to$ a Y_o or Y_1 propagator (see Eq. (7.2)). One has in this case an anomalous threshold in the t channel whose value is $1.73\mu^2$.

The Landau curves $t = t(s)$ are again used as in the case of πd scattering in order to study the analyticity properties of the amplitudes. To determine the curves, it is within the spirit of the two-complex-pole hypothesis to assume that Y_o and Y_1 can be treated as particles, and, indeed, for the sake of simplicity, we take them to be stable particles. The Landau curves are then determined from Eq. (3.3a), and are shown in Fig. 20 for the case of solution II (Eq. 7.5). For the case of solution I (Eq. (7.4)), the results will evidently be quite similar; for the sake of definiteness, we shall therefore consider only the type II solution.

As may be seen from Fig. 20, the s value corresponding to the anomalous threshold t_o appears in the physical region of s ($s \gtrsim$ normal threshold) for both Y_o and Y_1. Now, suppose that, as in the πd case, we determine the K^-d scattering amplitude in the unphysical region of the s channel (say, s small and positive); then we can continue this amplitude analytically into the physical region of the s channel. As discussed in detail in Sec. V, if s passes the point s_m corresponding to the anomalous threshold $t_o = t(s_m)$ in the process of the analytic continuation of the amplitude with respect to s, a continuation of the amplitude into the second sheet through the t branch cut which runs to the right of t_o becomes necessary. When we consider K^-d scattering at k = 105 MeV/c and 300 MeV/c, it is easily seen from Fig. 20 that the analytic continuation into the second t plane is necessary for all cases except when Y_1 is involved and k = 105 MeV/c.

It is now straightforward to obtain the K^-d scattering amplitude T(t,s) for fixed s ($> (d+m_k)^2$). The general procedure is very similar to the case of πd scattering and we therefore simply write down the result, retaining only the contribution from the anomalous region ($t \lesssim 4M^2$). For the case Y_o and k = 105 MeV/c and 300 MeV/c, the corresponding K^-d scattering amplitude $T_{Y_o}(t,s)$ becomes

$$T_{Y_0}(t,s) = \frac{g^2\Gamma_0^2}{16\pi}\left\{\int_{t_0}^{t(s)} \frac{dt'}{(t'-t)\sqrt{t'(t(s)-t')[s-(M+Y_0)^2][s-(M-Y_0)^2]}}\right.$$

$$\left. - i\int_{t(s)}^{4M^2} \frac{dt'}{(t'-t)\sqrt{t'(t'-t(s))[s-(M+Y_0)^2][s-(M-Y_0)^2]}}\right\}. \quad (7.6)$$

For the case Y_1 and k = 300 MeV/c, we obtain the same result as Eq. (7.6) for the amplitude except that $Y_o \to Y_1$. When we have Y_1 and k = 105 MeV/c, the corresponding amplitude $T_{Y_1}(t,s)$ assumes the form,

$$T_{Y_1}(t,s) = \frac{g^2 \Gamma_0^{2}}{16\pi} \left\{ -\int_{t_0}^{4M^2} \frac{dt'}{(t'-t)\sqrt{t'(t(s)-t')[s-(M+Y_1)^2][s-(M-Y_1)^2]}} \right\}. \tag{7.7}$$

The t' integrations can be carried out, and the angular dependences of $T_{Y_o, Y_1}(t,s)$ thus obtained are tabulated in Table III.

The total K^-d elastic scattering amplitude $T_i(t,s)$ may next be expressed in terms of T_{Y_o} and T_{Y_1}, viz.,

$$T_i(t,s) = \frac{1}{2} T_{Y_0}(t,s) + \frac{3}{2} T_{Y_1}(t,s),$$

from which one may proceed directly to find the angular distribution of the differential scattering cross section. The results are presented in Table IV and Figs. 21 and 22.

Since the experimental angular distributions for K^-d elastic scattering are not yet available, we can only compare our results with other calculations. At low energy there is fairly good agreement of the angular distribution with those obtained by Hetherington and Schick[29] in their phenomenological treatment of the problem.* On the other hand, at the higher energy, our cross sections are smaller than theirs; this is due mainly to the fact that our K^-p total cross section is smaller.

The total K^-d cross section can be calculated by means of the optical theorem and yields

103 mb at k = 105 MeV/c,

47 mb at k = 300 MeV/c,

to be compared with the results of Hetherington and Schick,

434 mb at k = 105 MeV/c,

96.2 mb at k = 300 MeV/c.

---

*The curves marked HS (I and II) in Figs. 21 and 22 are those of Hetherington and Schick in the impulse approximation.

In our impulse approximation, we have taken into account the contribution to the t integral from the anomalous region only ($t \lesssim 4M^2$). If the contribution from the normal region is large, then the imaginary part of the amplitude in the normal region should not be negligible. Thus, our result seems to indicate that the assumption that only the anomalous region is important may not be valid in the case of K^-d scattering.

While the two-complex-pole approximation which we have employed might be expected to include the effects of Figs. 5a and b, it is also of some interest to consider briefly the contributions of Figs. 5c and d to the scattering. Actually, Fig. 5c vanishes in our problem, and, from crossing symmetry, an analysis of Fig. 5d requires a knowledge of K^+N scattering. Unfortunately, we do not know the K^+N scattering length for the I = 0 state, and so we can only estimate the effect due to K^+N scattering in the I = 1 state. Since the energy dependence of the I = 1 scattering cross section is very small at low energies, we may regard Fig. 5d as a triangle diagram. In terms of the K^+N scattering length B_1, the K^-d scattering amplitude $T_i(t)$ for the diagram becomes (see Eq. (4.20))

$$T_i(t) = -\Gamma_0{}^2 B_1 \int_{t_0}^{4M^2} \frac{dt'\,(M+m_K)}{(t'-t)\sqrt{t'(4d^2-t')}} \; . \tag{7.8}$$

With B_1 = -0.30 F, one can show that the effect of $T_i(t)$ on $T_i(t,s)$ is to decrease the cross section somewhat in the forward direction at low energy. At higher energies, the resultant cross section will generally increase, particularly, in the forward direction. Although one does not have enough information to carry out an accurate calculation at this time, the effect would appear to improve upon the impulse approximation.

VIII. CONCLUSION

We have developed a procedure within the framework of S-matrix theory for studying the scattering of mesons by deuterons at low energy. In the development of the formalism, the recognition of the fact that a deuteron is a loosely bound state of a proton and a neutron leads to a great deal of simplification. An immediate consequence of this is the appearance of small anomalous thresholds in the t channel, which makes the use of t-channel unitarity more convenient than the s-channel unitarity conventionally used. A second consequence is that it is reasonable to assume at the energies in question that the contribution to the meson-deuteron scattering amplitude from the anomalous region dominates that from the normal region and that a study of the amplitude in terms of selected diagrams is justified. Under these assumptions the properties of triangle and box diagrams, including various mesonic corrections, have been determined from the requirements of unitarity and analyticity. In particular, we have found that the binding-correction and multiple-scattering terms are characterized by the anomalous parts of the deuteron-baryon vertices and that the double-scattering amplitudes have no complex singularities. The t dispersion relations have been obtained for these amplitudes by the method of analytic continuation with respect to the deuteron mass and with respect to s.

By way of application, the angular distributions of π^+d and K^-d elastic scattering have been calculated. In the former case, the N^* binding-correction terms seem to be the main correction to the impulse approximation, and they are in the right direction. The multiple-scattering corrections diminish rapidly in their significance as the number of intermediate-state particles increases.

While the essential point of the formalism is that it enables one to treat seriously the effects of diagrams involving many-particle (up to four) intermediate states, it is perhaps well to emphasize that the specific calculations which have been carried out were based on spinless particles and so can only suggest the results of a more realistic model.

We have concerned ourselves with elastic meson-deuteron scattering. The extension of the formalism so that it includes inelastic phenomena is important but it is not trivial. Ultimately, one may be able to give a unified treatment of both types of processes by invoking generalized unitarity leading to coupled integral equations for the system, but this approach lies beyond the scope of this paper.

REFERENCES

1. E. E. Salpeter and H. A. Bethe, Phys. Rev. 84, 1232 (1951).
2. M. Gell-Mann and F. E. Low, Phys. Rev. 84, 350 (1951).
3. S. S. Schweber, Relativistic Quantum Field Theory (Row, Peterson and Co., Evanston, Illinois, 1961).
4. J. M. Blatt and V. F. Weisskopf, Theoretical Nuclear Physics (John Wiley and Sons, Inc., New York, 1952).
5. G. F. Chew, Phys. Rev. 80, 196 (1950).
6. G. F. Chew and G. C. Wick, Phys. Rev. 85, 636 (1952).
7. G. F. Chew and M. L. Goldberger, Phys. Rev. 87, 778 (1952).
8. S. Fernbach, F. A. Green, and K. M. Watson, Phys. Rev. 82, 980 (1951); 84, 1084 (1951).
9. R. L. Gluckstern and H. A. Bethe, Phys. Rev. 81, 761 (1951).
10. H. A. Bethe and F. de Hoffmann, Mesons and Fields II (Row, Peterson and Co., Evanston, Illinois, 1955).
11. J. Ashkin, J. B. Blazer, F. Feiner, J. G. Gorman, and M. O. Stern, Phys. Rev. 96, 1104 (1954).
12. D. E. Nagle, Phys. Rev. 97, 480 (1955).
13. A. E. Ignatenko et al., Dok. Akad. Nauk SSSR 103, 209 (1955).
14. E. Arase, G. Goldhaber, and S. Goldhaber, Phys. Rev. 90, 160 (1953).
15. K. C. Rogers and L. M. Lederman, Phys. Rev. 105, 247 (1957).
16. R. M. Rockmore, Phys. Rev. 105, 256 (1957).
17. K. A. Brueckner, Phys. Rev. 89, 834 (1953); 90, 715 (1953).
18. S. D. Drell and L. Verlet, Phys. Rev. 99, 849 (1955).
19. V. DeAlfaro and R. Straffolini, Nuovo Cimento 11, 447 (1959).
20. B. H. Bransden and R. G. Moorhouse, Nucl. Phys. 6, 310 (1958).

21. E. G. Pewitt et al., Phys. Rev. 131, 1826 (1963).

22. H. N. Pendleton, Phys. Rev. 131, 1833 (1963).

23. E. Ferreira, Phys. Rev. 115, 1727 (1959).

24. L. Alvarez, Proceedings of the Ninth International Conference on High Energy Physics, Kiev, 1959 (unpublished).

25. N. Horwitz, private communication.

26. T. B. Day, G. A. Snow, and J. Sucher, University of Maryland Tech. Rep. No. 142 (1959); Nuovo Cimento 13, 614 (1959); Phys. Rev. 119, 1110 (1960).

27. A. K. Bhatia and J. Sucher, Phys. Rev. 132, 855 (1963).

28. R. Chand, Ann. Phys. (N. Y.) 22, 438 (1963); Nuovo Cimento 31, 827 (1964).

29. J. H. Hetherington and L. H. Schick, Phys. Rev. 137, B935 (1964).

30. J. J. Brehm and J. Sucher, Ann. Phys. (N. Y.) 25, 1 (1963); J. J. Brehm, Ann. Phys. (N. Y.) 25, 221 (1963).

31. S. Mandelstam, Proceedings of the Fourth Annual Eastern Theoretical Physics Conference, Stony Brook, 1965 (to be published); Phys. Rev. 140, B375 (1965).

32. G. F. Chew, S-Matrix Theory of Strong Interactions (W. A. Benjamin, Inc., New York, 1961).

33. F. Kaschluhn, Z. Naturforsch. 13a, 183 (1958); Nucl. Phys. 8, 303 (1958); 9, 347 (1959).

34. M. Gell-Mann, M. L. Goldberger, and W. Thirring, Phys. Rev. 95, 1612 (1954); M. L. Goldberger, Phys. Rev. 99, 979 (1955).

35. M. L. Goldberger, M. Miyazawa, and R. Oehme, Phys. Rev. 99, 986 (1955).

36. J. D. Jackson, Dispersion Relations (Interscience Publishers, Inc., New York, 1961), edited by G. R. Screaton.

37. S. W. MacDowell, Phys. Rev. 116, 774 (1960).

38. G. F. Chew and S. Mandelstam, Phys. Rev. 119, 467 (1960); UCRL-9126.

39. See the articles in Ref. 36 by M. J. Moravcsik and by W. R. Frazer.

40. R. E. Cutkosky, J. Math. Phys. 1, 429 (1960).

41. R. Blankenbecler, Phys. Rev. 122, 983 (1960).

42. S. Mandelstam, Phys. Rev. 112, 1344 (1958); 115, 1741, 1752 (1959).

43. J. C. Polkinghorne, Nuovo Cimento 23, 360; 25, 1 (1962).

44. S. Mandelstam, Phys. Rev. Letters 4, 84 (1960).

45. R. Blankenbecler and Y. Nambu, Nuovo Cimento 18, 595 (1960).

46. V. N. Gribov and I. T. Dyatlov, Soviet Phys.—JETP 15, 140 (1962).

47. R. Oehme, Werner Heisenberg und die Physik Unserer Zeit (F. Vieweg und Sohn, Braunschweig, 1961), p. 240.

48. P. T. Matthews, Lectures on Strong and Electromagnetic Interactions, Brandeis University, 1963, p.1.

49. K. Symanzik, Phys. Rev. 105, 745 (1957).

50. N. Bogoliubov, M. Medvedev, and M. Polivanov, Fortschritte der Physik 6, 169 (1958).

51. H. Bremermann, R. Oehme, and J. G. Taylor, Phys. Rev. 109, 2178 (1958).

52. H. Lehmann, Nuovo Cimento 10, 579 (1958).

53. H. Lehmann, Nuovo Cimento (Suppl.) 14, 153 (1959).

54. R. J. Eden, Brandeis Lectures in Theoretical Physics, 1961 (W. A. Benjamin, Inc., New York, 1962), vol. I, p. 1.

55. R. J. Eden, Phys. Rev. 119, 1763 (1960); 120, 1514 (1960); 121, 1567 (1960).

56. P. V. Landshoff, J. C. Polkinghorne, and J. C. Taylor, Nuovo Cimento 19, 939 (1961).

57. N. Nakanishi, Prog. Theoret. Phys. (Suppl.) 18, 1 (1961).

58. J. C. Polkinghorne and G. R. Screaton, Nuovo Cimento 15, 289 (1960).

59. J. Tarski, J. Math. Phys. 1, 149 (1960).

60. L. Landau, Nucl. Phys. 13, 181 (1959).

61. J. D. Bjorken, Ph.D. thesis, Stanford University, 1959 (unpublished).

62. D. I. Olive, Nuovo Cimento 26, 73 (1962).

63. H. P. Stapp, Phys. Rev. 125, 2139 (1962).

64. J. D. Bjorken and S.D.Drell, Relativistic Quantum Fields (McGraw-Hill Book Co., New York, 1965).

65. R. Karplus, C. M. Sommerfield, and E. H. Wichmann, Phys. Rev. 114, 376 (1959).

66. R. Karplus, C. M. Sommerfield, and E. H. Wichmann, Phys. Rev. 111, 1187 (1958).

67. J. C. Taylor, Phys. Rev. 117, 261 (1960).

68. J. N. Islam and Y. S. Kim, Phys. Rev. 138, 1222 (1965).

69. R. J. Eden, P. V. Landshoff, J. C. Polkinghorne, and J. C. Taylor, J. Math. Phys. 2, 656 (1961).

70. R. E. Cutkosky, Proceedings of the 1960 International Annual Conference on High Energy Physics at Rochester (Interscience Publishers, Inc., New York, 1960), p. 236.

71. F. Gross, Phys. Rev. 134, B405 (1964); 140, B410 (1965).

72. R. Blankenbecler, M. L. Goldberger, S. W. MacDowell, and S. B. Treiman, Phys. Rev. 123, 692 (1961).

73. L. F. Cook, Jr. and B. W. Lee, Phys. Rev. 127, 283, 297 (1962).

74. J. S. Ball, W. R. Frazer, and M. Nauenberg, Phys. Rev. 128, 478 (1962).

75. U. Haber-Schaim, Phys. Rev. 104, 1113 (1956).

76. R. H. Dalitz, Strange Particles and Strong Interactions (Oxford University Press, 1962).

77. R. H. Dalitz and S. F. Tuan, Ann. Phys.(N. Y.) 10, 307 (1960).

78. W. R. Humphrey and R. R. Ross, Phys. Rev. 127, 1305 (1962).

79. R. R. Ross, UCRL-9749.

80. S. Goldhaber, Phys. Rev. Letters 9, 135 (1962).

TABLE I

Angular dependence of the π^+d scattering amplitude at 85 MeV, with and without binding corrections of the type given in Figs. 17a and b. The angles are in the center-of-mass system. The f's are evaluated in units of $1/\mu$.

$\cos\theta$	f_{i1}	f_{b1}	f_i	$f_i + f_{b1}$
1	-0.0729 + 0.0141i	0.0063 - 0.0044i	0.555 + 0.115i	0.561 + 0.111i
0.5	-0.0588 + 0.0205i	0.0061 - 0.0043i	0.574 + 0.108i	0.580 + 0.104i
0	-0.0508 + 0.0250i	0.0059 - 0.0042i	0.557 + 0.107i	0.563 + 0.103i
-0.5	-0.0448 + 0.0314i	0.0057 - 0.0042i	0.512 + 0.108i	0.518 + 0.104i
-1	-0.0408 + 0.0429i	0.0055 - 0.0041i	0.501 + 0.116i	0.507 + 0.112i

TABLE II

Angular dependence of the π^+d scattering amplitude at 85 MeV with binding corrections of the type given in Figs. 17c and d. The angles are in the center-of-mass system. The f's are evaluated in units of $1/\mu$.

$\cos\theta$	f_{b2}	$f_i + f_{b2}$
1	-0.0596 + 0.0416i	0.495 + 0.157i
0.5	-0.0577 + 0.0409i	0.516 + 0.149i
0	-0.0558 + 0.0402i	0.501 + 0.147i
-0.5	-0.0540 + 0.0396i	0.458 + 0.148i
-1	-0.0524 + 0.0390i	0.449 + 0.155i

TABLE III

Angular dependences of the K^-d scattering amplitudes $T_{Y_o}(t,s)$ and $T_{Y_1}(t,s)$ at (a) k = 105 MeV/c ($s = 290\mu^2$) and (b) k = 300 MeV/c ($s = 304\mu^2$). The angles are in the center-of-mass system; $T/(g^2\Gamma_o^2)$ is expressed in units of $1/\mu^4$.

$\cos\theta$	$T_{Y_o}(t,s)/(g^2\Gamma_o^2/16\pi)$	$T_{Y_1}(t,s)/(g^2\Gamma_o^2/16\pi)$
	(a)	
1	0.0149 - 0.0088i	-0.0383
0.5	0.0135 - 0.0085i	-0.0353
0	0.0124 - 0.0082i	-0.0327
-0.5	0.0115 - 0.0080i	-0.0307
-1	0.0107 - 0.0077i	-0.0289
	(b)	
1	0.0053 - 0.0020i	0.0068 - 0.0031i
0.5	0.0033 - 0.0017i	0.0042 - 0.0026i
0	0.0025 - 0.0015i	0.0031 - 0.0022i
-0.5	0.0020 - 0.0015i	0.0025 - 0.0020i
-1	0.0017 - 0.0013i	0.0020 - 0.0018i

TABLE IV

Angular dependences of the K^-d scattering amplitude T_i (t,s) at (a) k = 105 MeV/c and (b) k = 300 MeV/c. The angles are in the center-of-mass system; $T/(g^2\Gamma_o{}^2)$ is expressed in units of $1/\mu^4$.

cos θ	$T_i\ (t,s)/(g^2\Gamma_o{}^2/16\pi)$
	(a)
1	-0.050 - 0.0044i
0.5	-0.046 - 0.0043i
0	-0.043 - 0.0041i
-0.5	-0.040 - 0.0040i
-1	-0.038 - 0.0039i
	(b)
1	0.0129 - 0.0057i
0.5	0.0080 - 0.0048i
0	0.0059 - 0.0042i
-0.5	0.0047 - 0.0037i
-1	0.0040 - 0.0034i

FIGURE CAPTIONS

Fig. 1. Diagram illustrating the reactions s: $1 + 2 \rightarrow 3 + 4$; t: $1 + \bar{3} \rightarrow \bar{2} + 4$; u: $1 + \bar{4} \rightarrow \bar{2} + 3$, as well as the corresponding inverse antiparticle reactions.

Fig. 2. The physical values of the invariants (shaded areas) in the s, t, and u channels for meson-deuteron scattering.

Fig. 3. A box diagram and several of its reduced diagrams.

Fig. 4. Schematic diagrams for meson-deuteron scattering; the dotted, solid, and double-solid lines represent mesons, baryons, and deuterons, respectively.

Fig. 5. Several Feynman diagrams corresponding to Fig. 4a.

Fig. 6. Reduced diagrams of Fig. 5a and their duals.

Fig. 7. Landau curves corresponding to Figs. 5a and b.

Fig. 8. Several Feynman diagrams corresponding to Fig. 4a; the values of the anomalous thresholds t_o are also given.

Fig. 9. (a,b) Binding, (c,d) double-scattering, and (e) triple-scattering corrections and some of the corresponding duals.

Fig. 10. (a) The impulse approximation for K^-d scattering; (b,c) double-scattering diagrams for K^-d scattering (Eq. 4.4).

Fig. 11. Contour modification due to an anomalous threshold (see Eq. (4.13)).

Fig. 12. A one-nucleon exchange approximation of $G(u,\xi)$.

Fig. 13. The binding corrections (a), (b), and (b'), and the triple-scattering corrections (c) and (c') for the case of generalized box diagrams.

Fig. 14. A typical Landau curve $t = t_+(s,\xi)$ for a binding-correction term (ξ fixed).

Fig. 15. The singularities $t_\pm(s)$ near $s = s_+^e$.

Fig. 16. The singularity $t_+(s)$ near $s = s_m$.

Fig. 17. Binding corrections to the impulse approximation for π^+d scattering.

Fig. 18. Angular distribution for π^+d elastic scattering at 85 MeV.

Fig. 19. Energy dependence of the K^-p elastic-scattering cross section in the two-complex-pole approximation (see Eqs. (7.4) and (7.5); the experimental points are taken from Ref. 79).

Fig. 20. Landau curves for K^-d scattering according to Fig. 5a ($s' \to Y_o, Y_1$ as given by solution II (Eq. 7.5)).

Fig. 21. Angular distribution for K^-d elastic scattering at k = 105 MeV/c.

Fig. 22. Angular distribution for K^-d elastic scattering at k = 300 MeV/c.

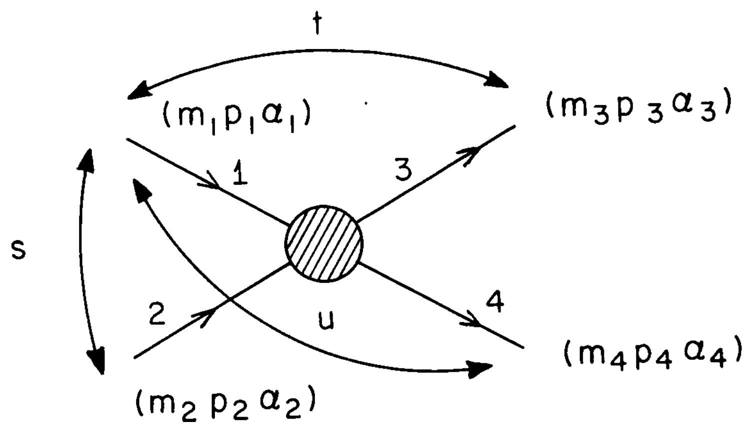

Fig. 1

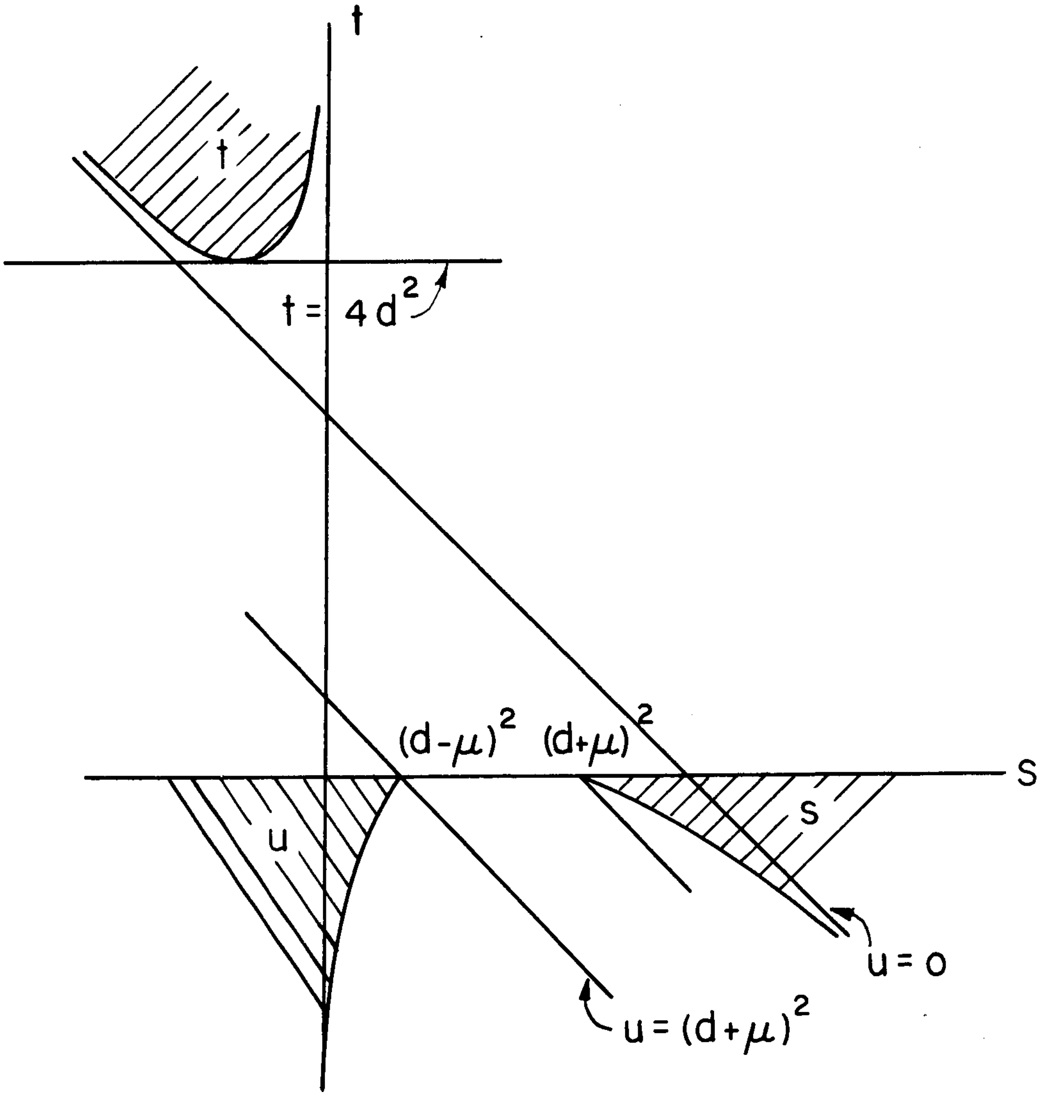

Fig. 2

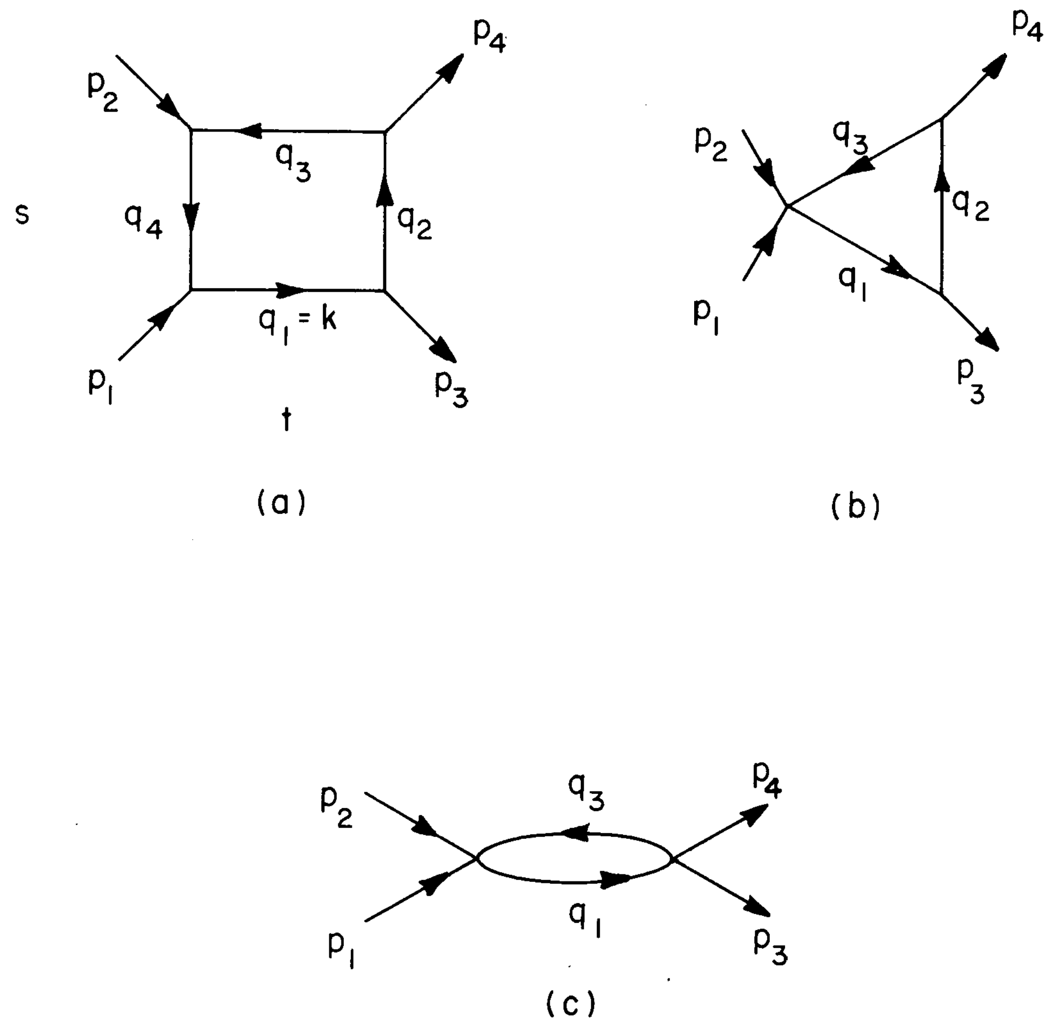

Fig. 3

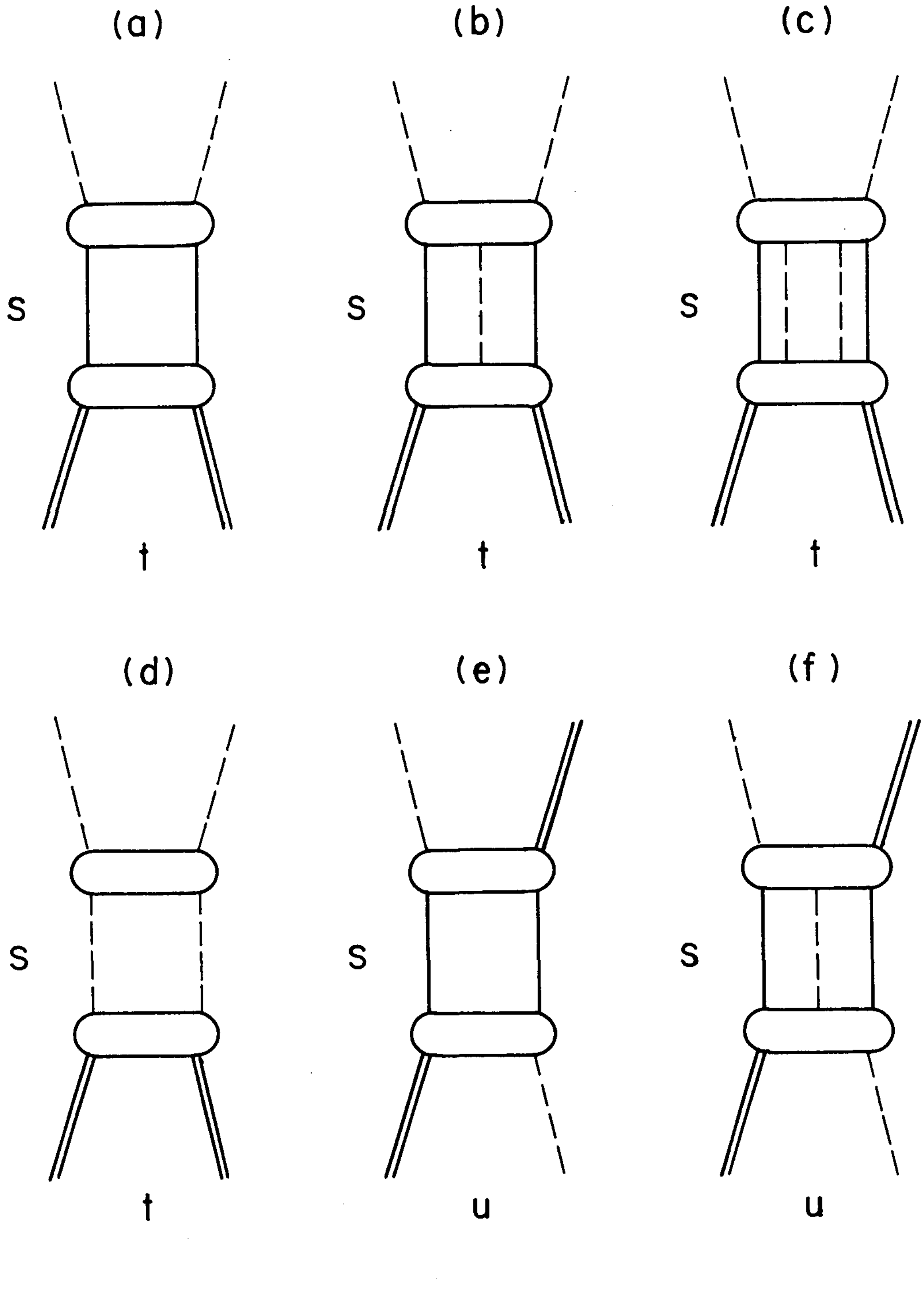

Fig. 4

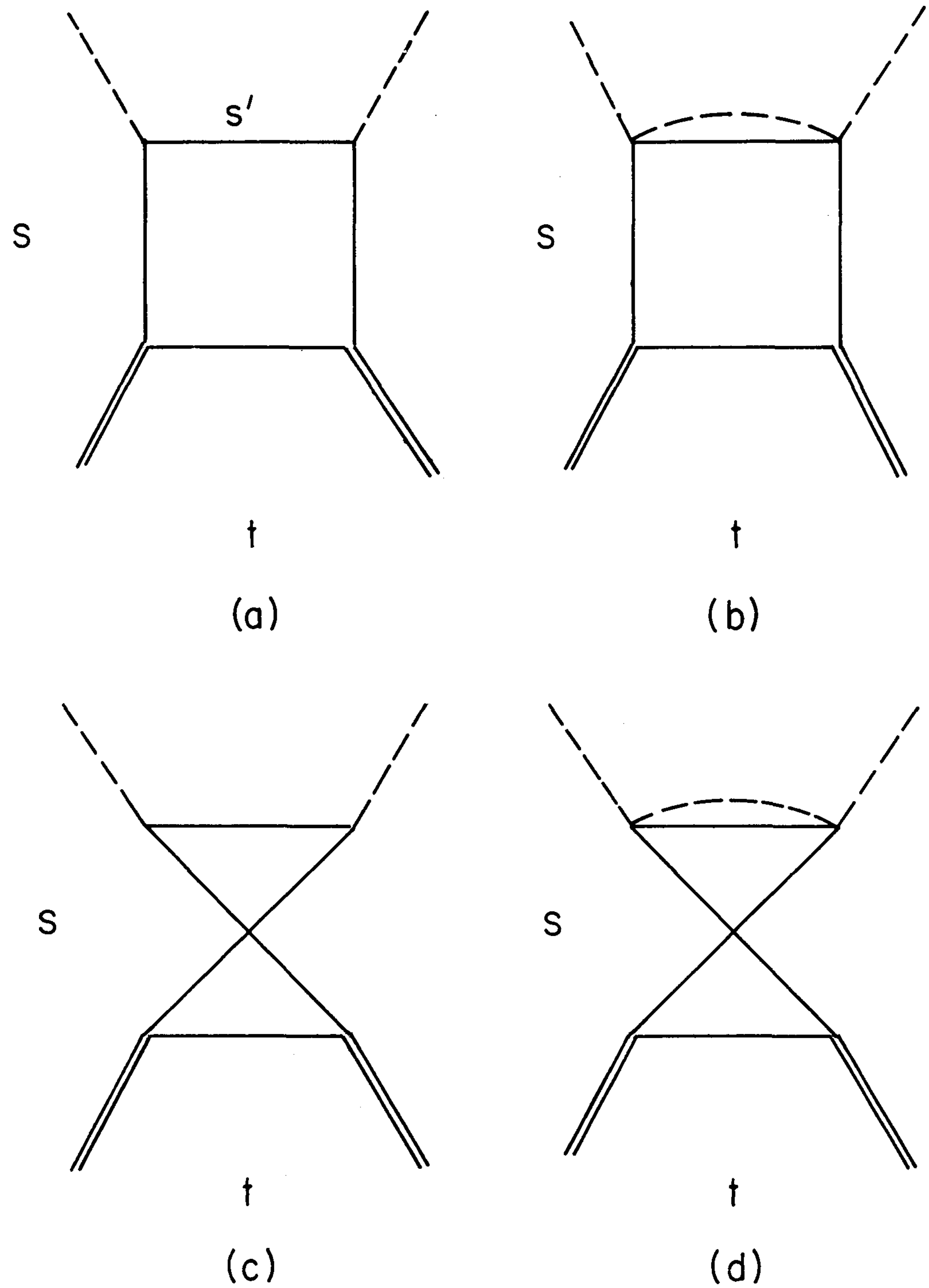

Fig. 5

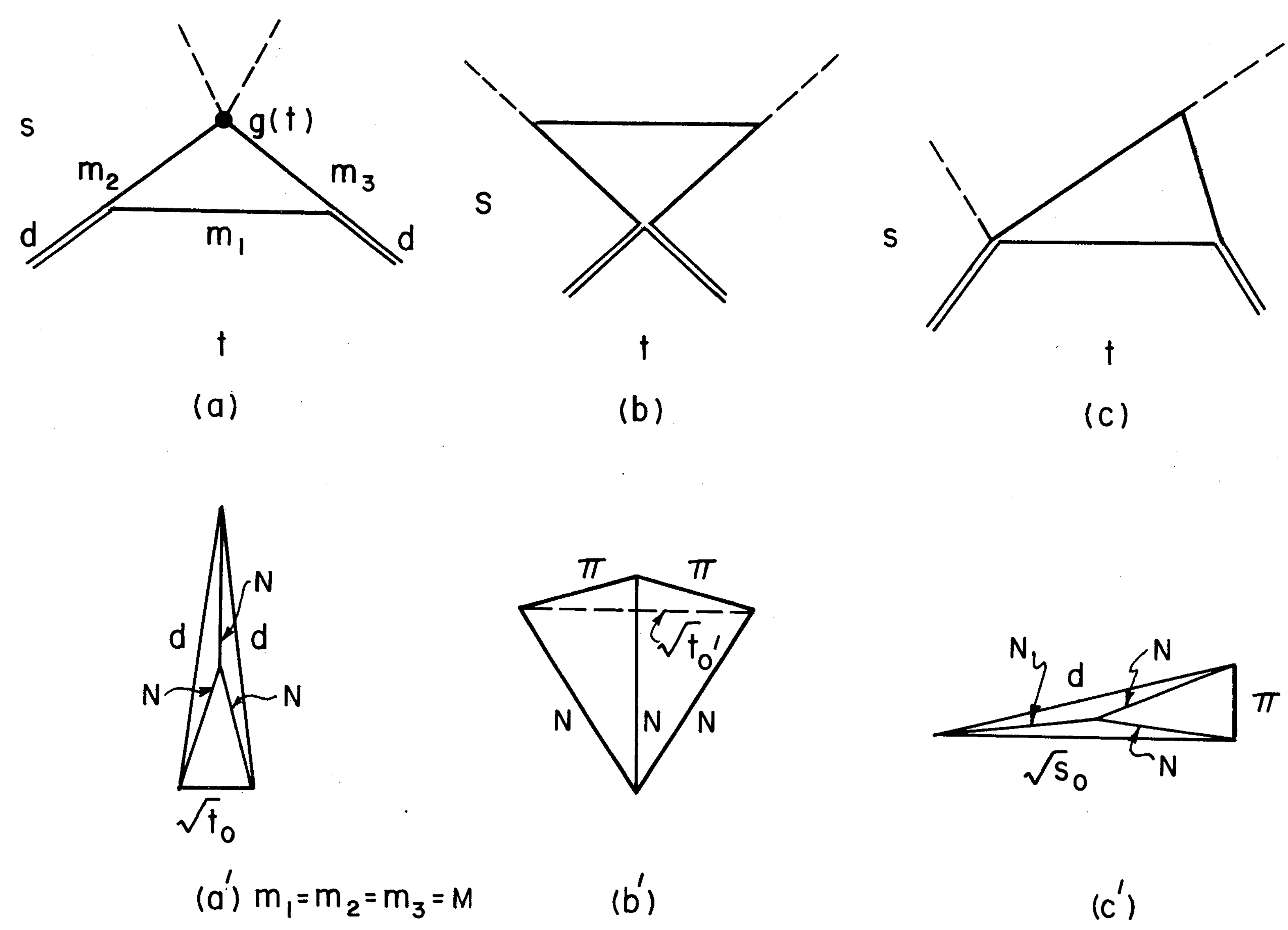
s
g(t)
m_2
m_3
d
m_1
d
t
(a)
s
t
(b)
s
t
(c)
N
d
d
N
N
$\sqrt{t_0}$
(a′) $m_1 = m_2 = m_3 = M$
π
π
$\sqrt{t_0'}$
N
N
N
(b′)
N_1
d
N
π
$\sqrt{s_0}$
N
(c′)

Fig. 6

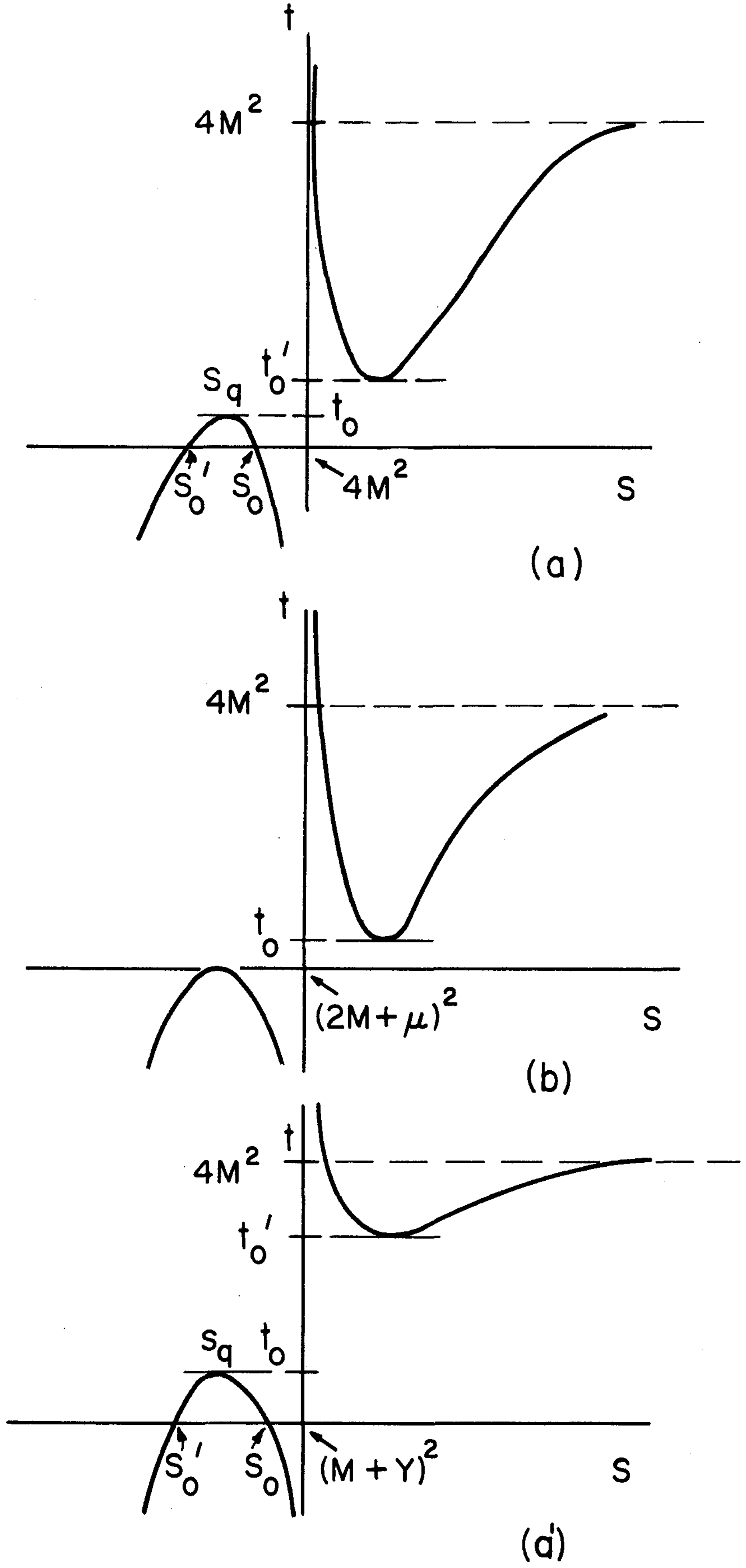

t
4M²
t₀′
S_q
t₀
S₀′
S₀
4M²
S
(a)
t
4M²
t₀
(2M+μ)²
S
(b)
t
4M²
t₀′
S_q
t₀
S₀′
S₀
(M+Y)²
S
(a′)

Fig. 7

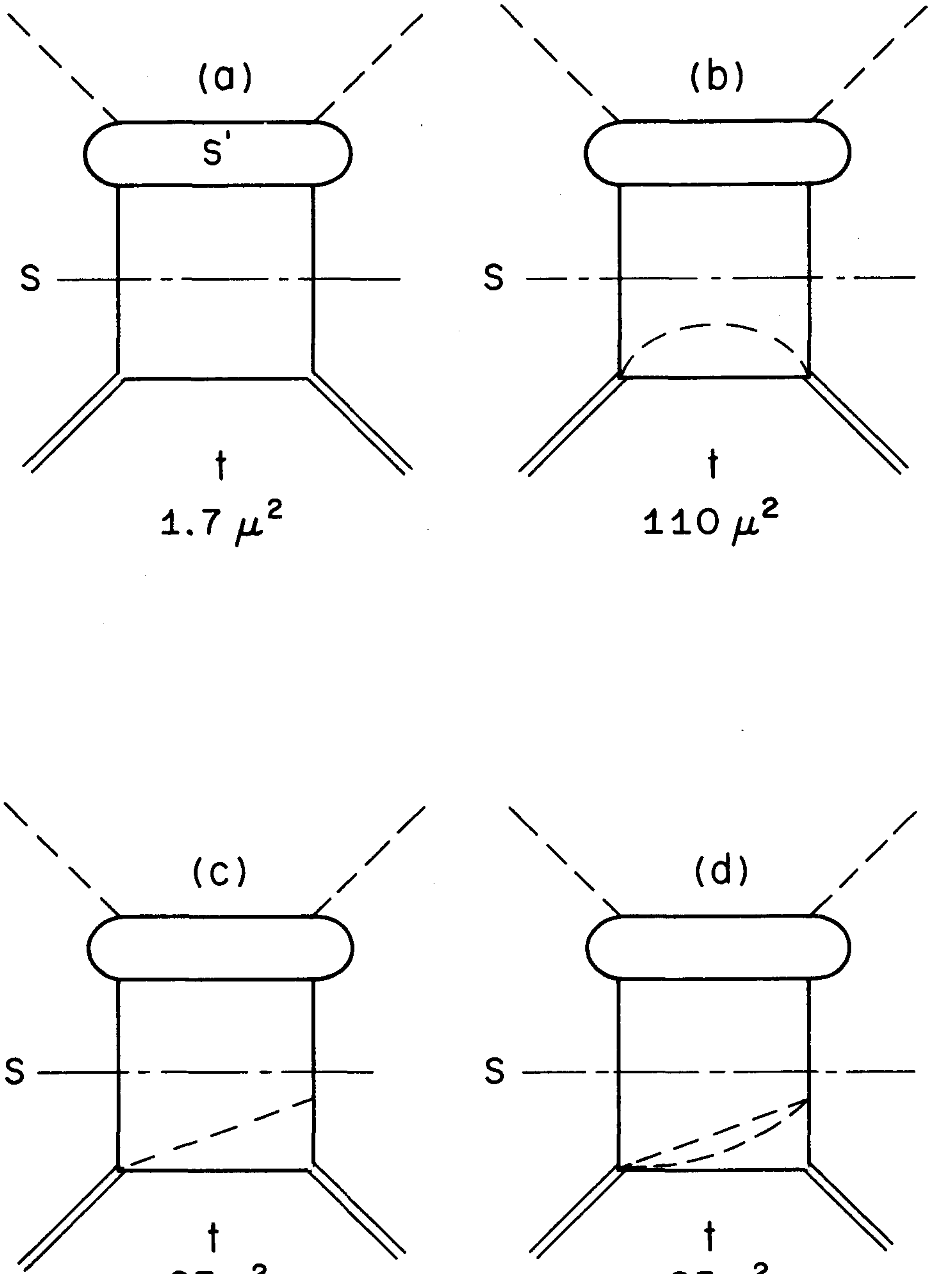

Fig. 8

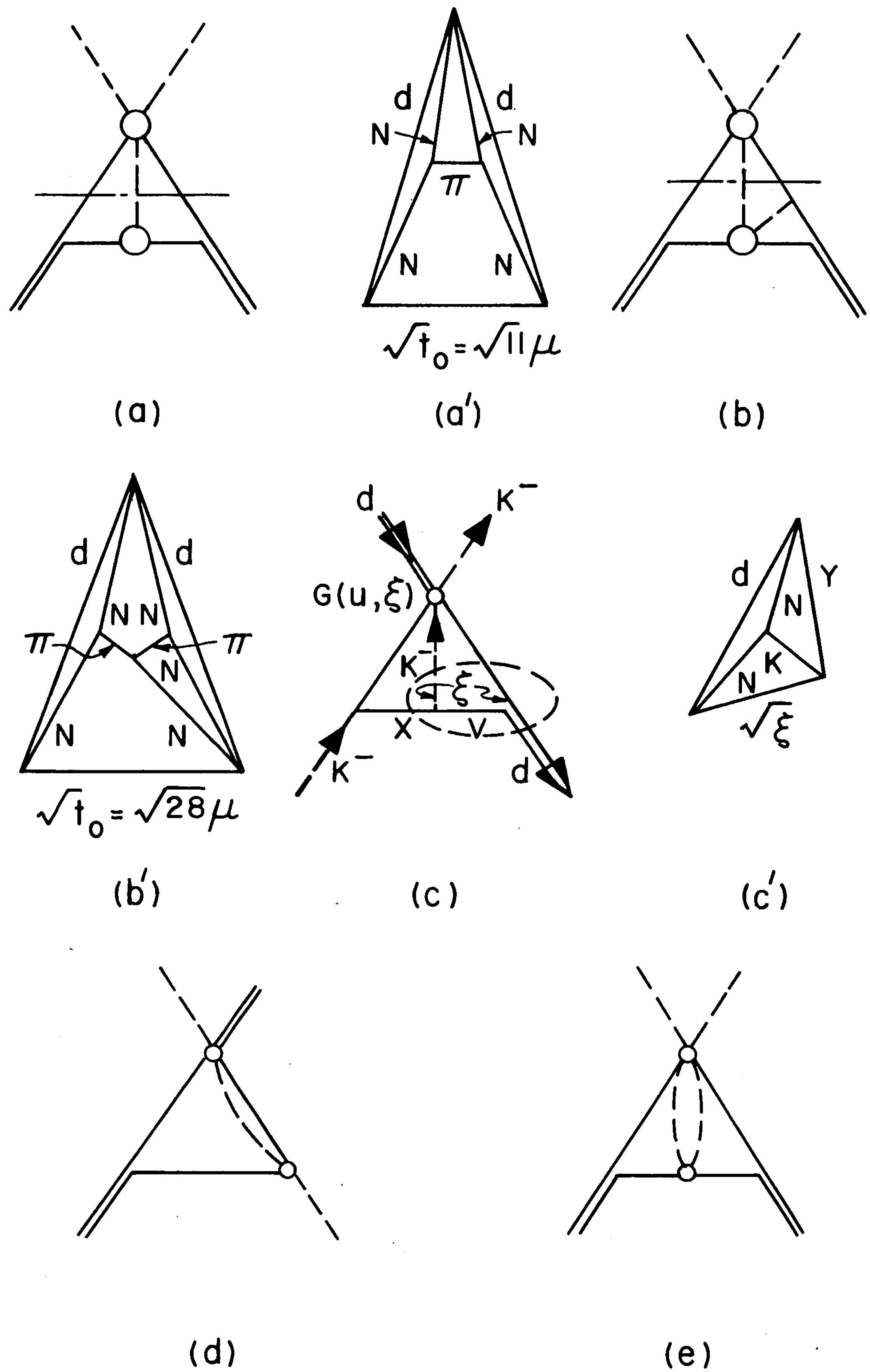

d
d
N
N
π
N
N
√t₀ = √11 μ
(a)
(a′)
(b)
d
d
N N
π
π
N
N
N
√t₀ = √28 μ
d
K⁻
G(u,ξ)
K⁻
ξ
X
V
K⁻
d
d
Y
N
K
N
√ξ
(b′)
(c)
(c′)
(d)
(e)

Fig. 9

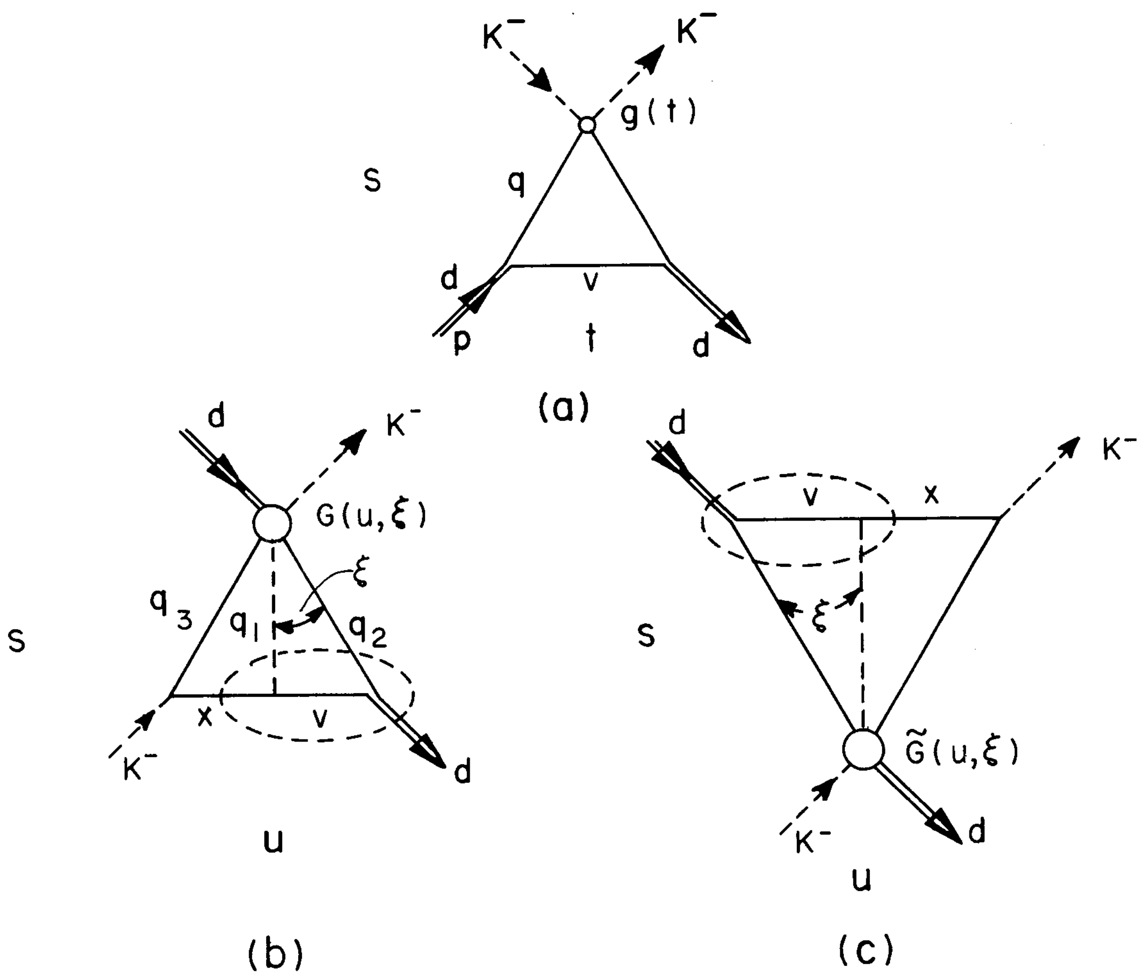

Fig. 10

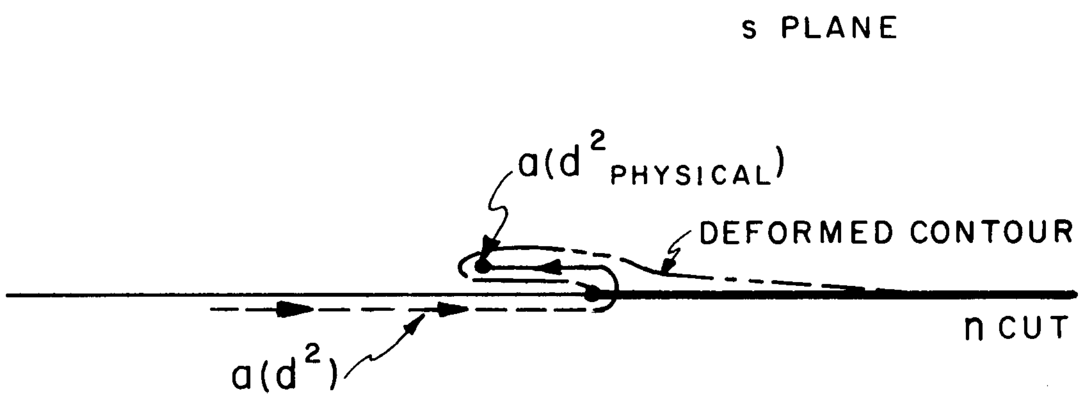

Fig. 11

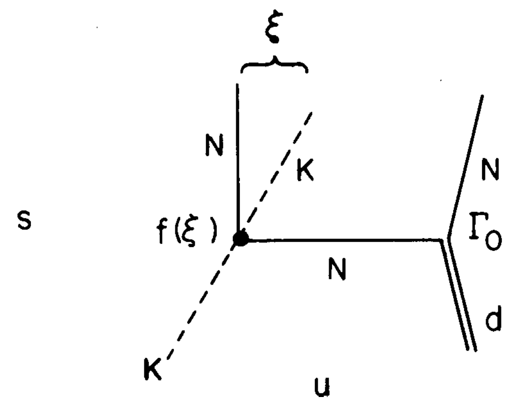

Fig. 12

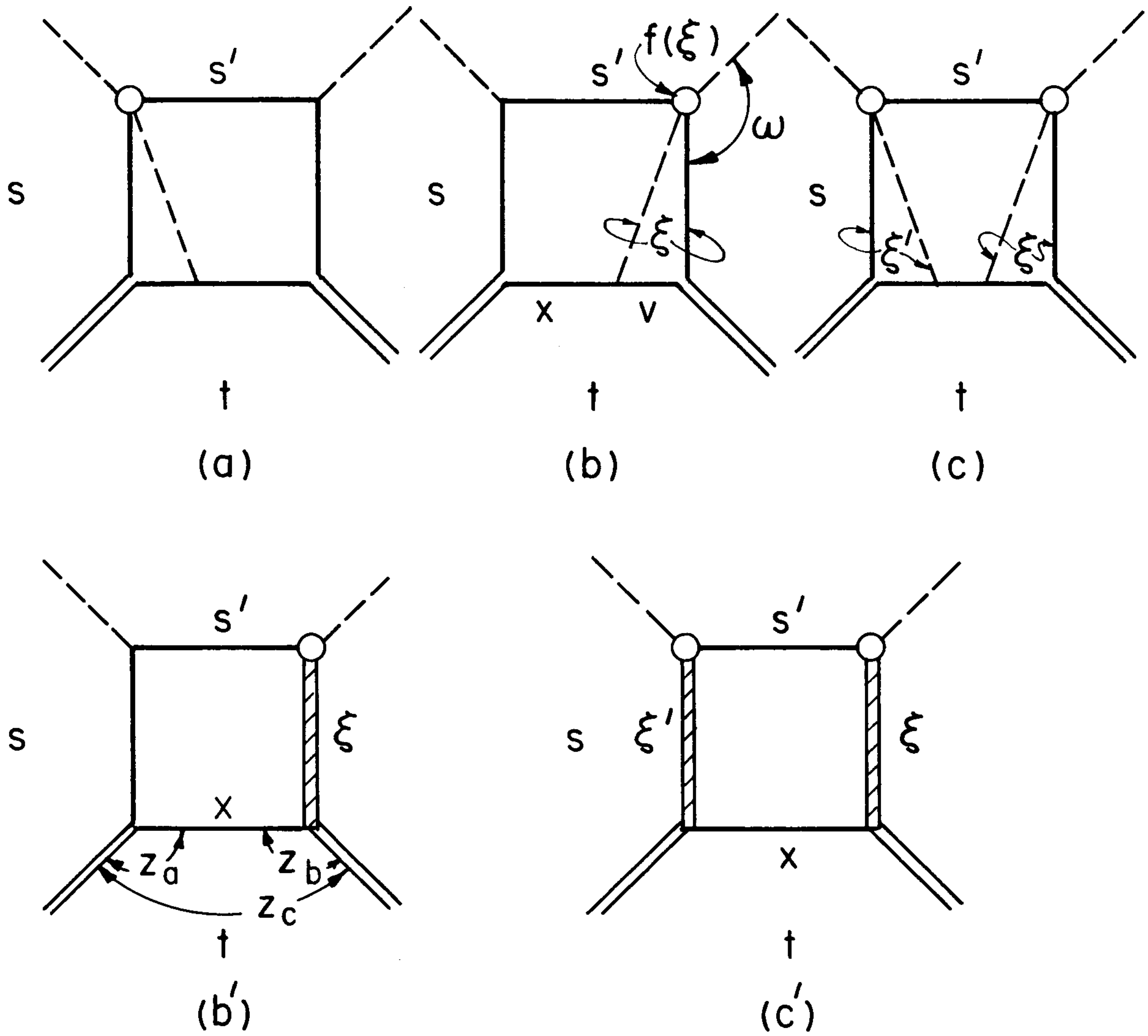

Fig. 13

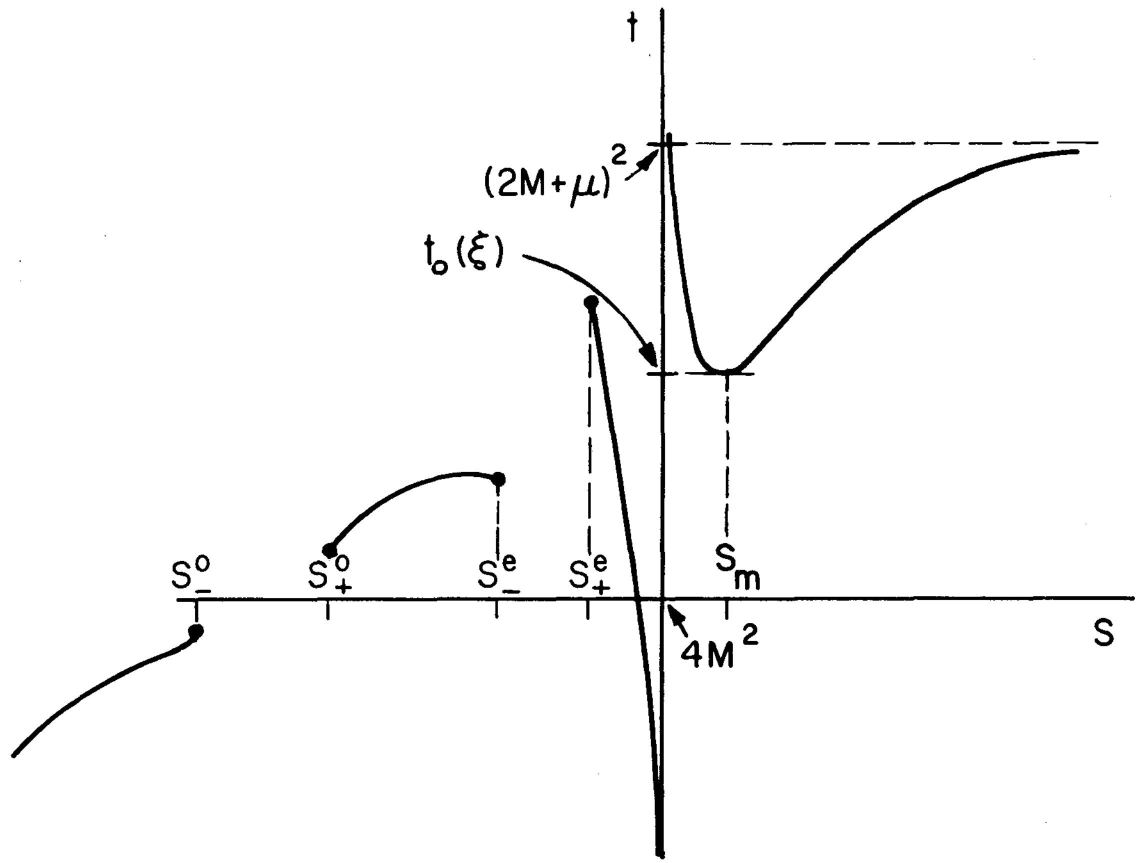

Fig. 14

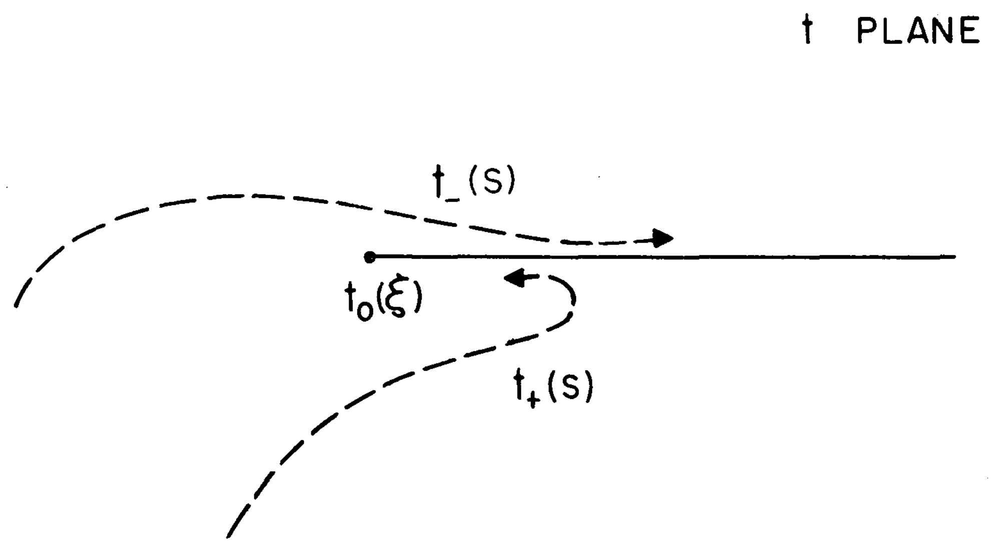

Fig. 15

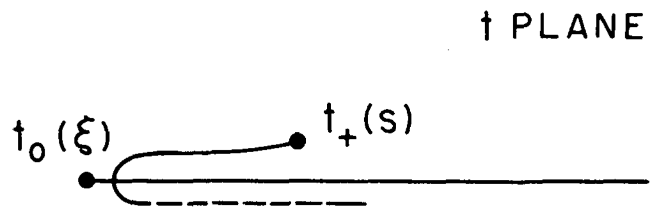

Fig. 16

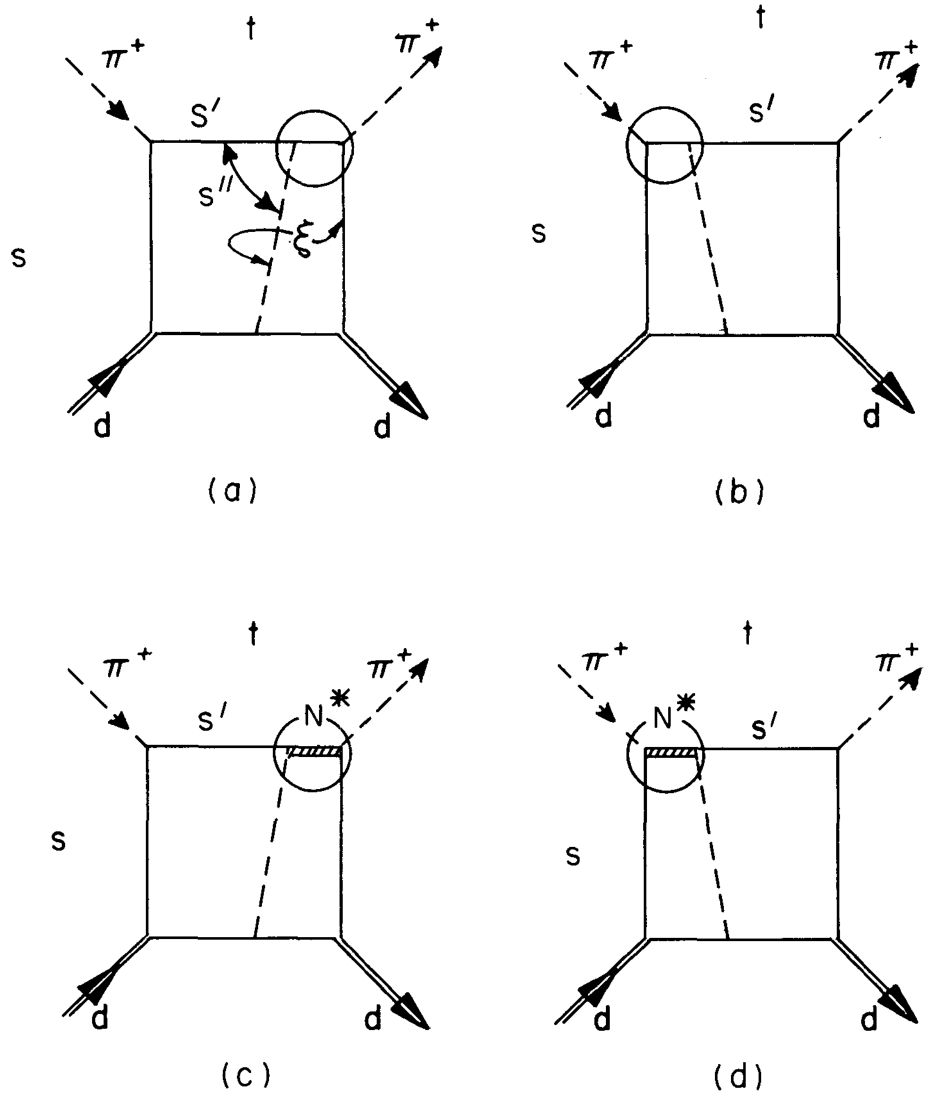

Fig. 17

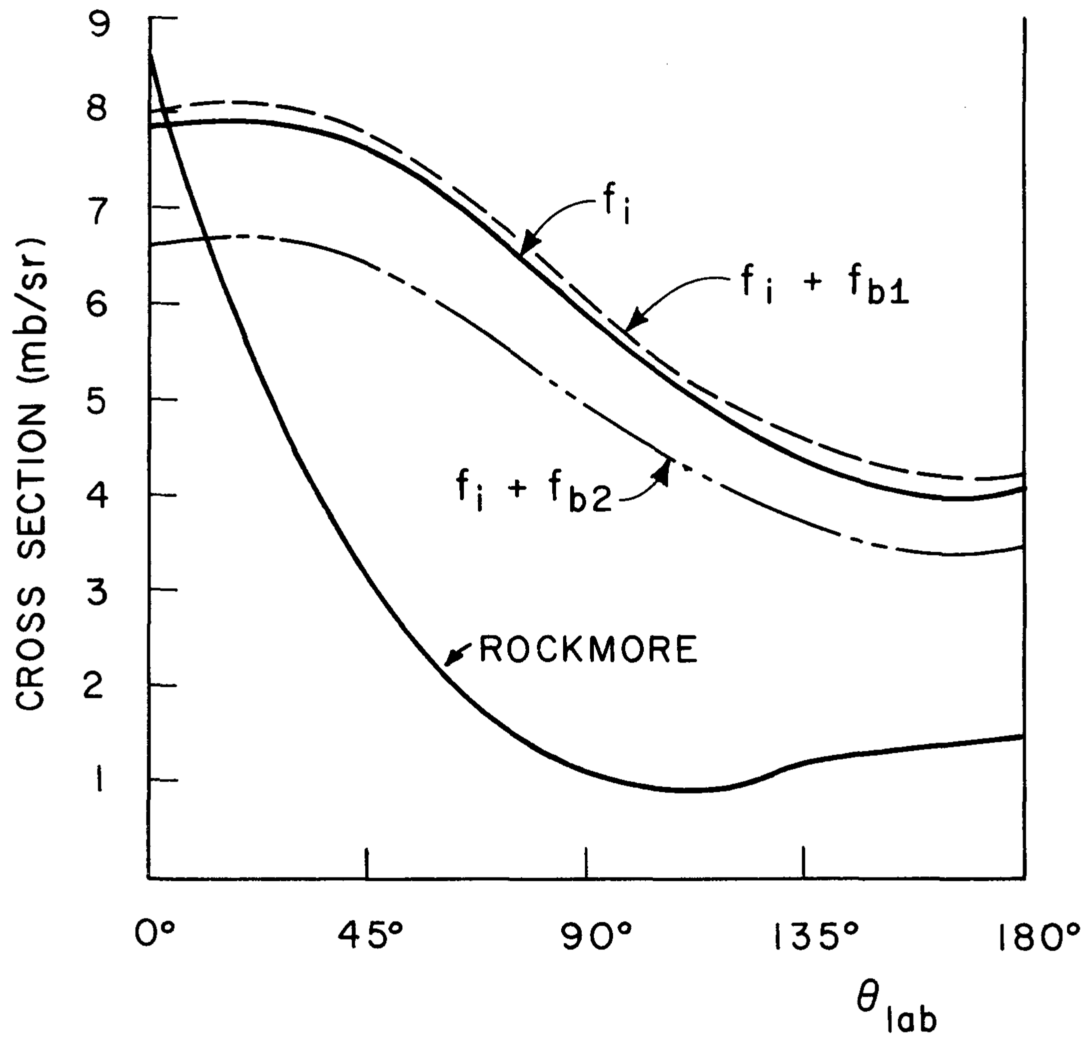
CROSS SECTION (mb/sr)
9
8
7
6
5
4
3
2
1
0°
45°
90°
135°
180°
θ_{lab}
f_i
$f_i + f_{b1}$
$f_i + f_{b2}$
ROCKMORE

Fig. 18

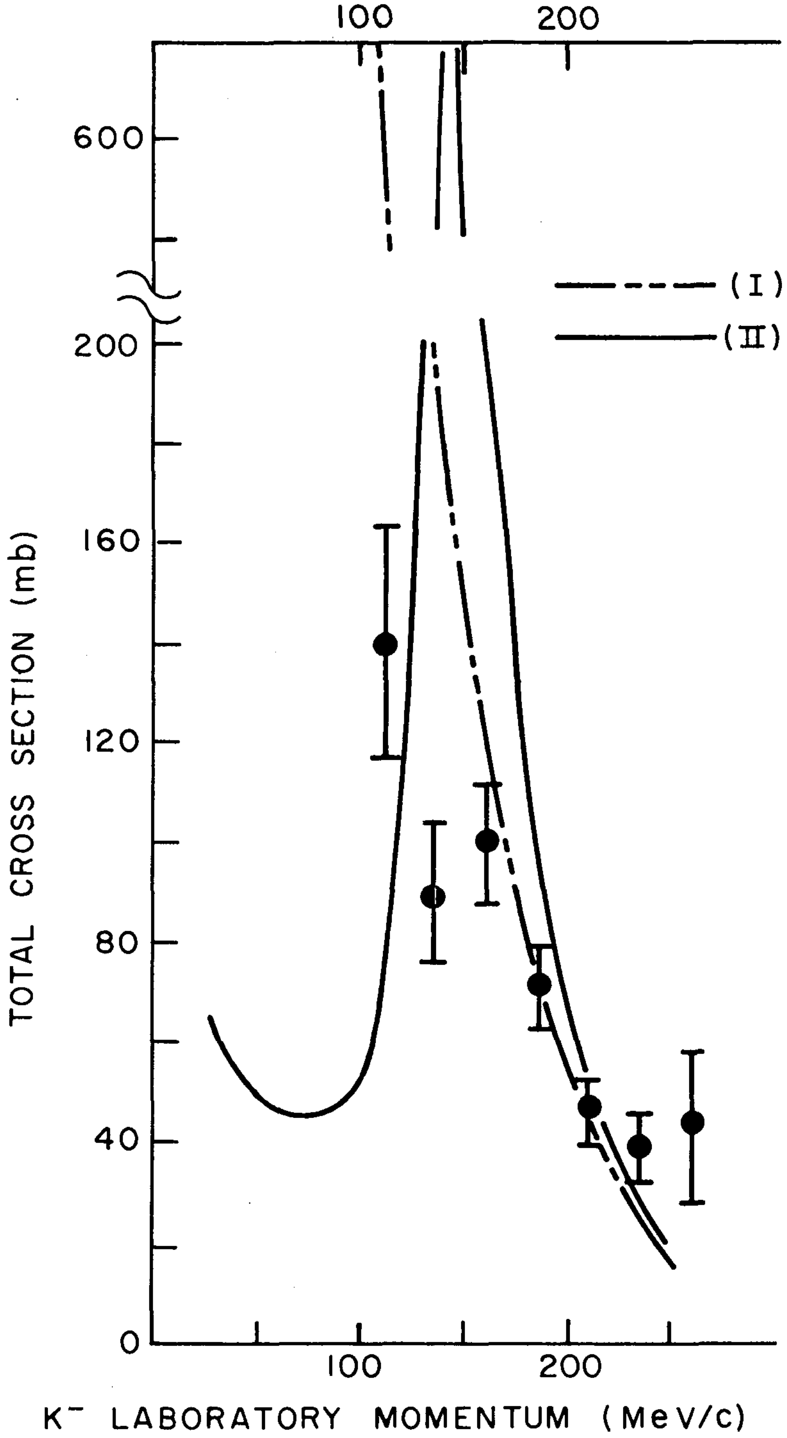
100
200
600
200
160
120
80
40
0
100
200
(I)
(II)
TOTAL CROSS SECTION (mb)
K⁻ LABORATORY MOMENTUM (MeV/c)

Fig. 19

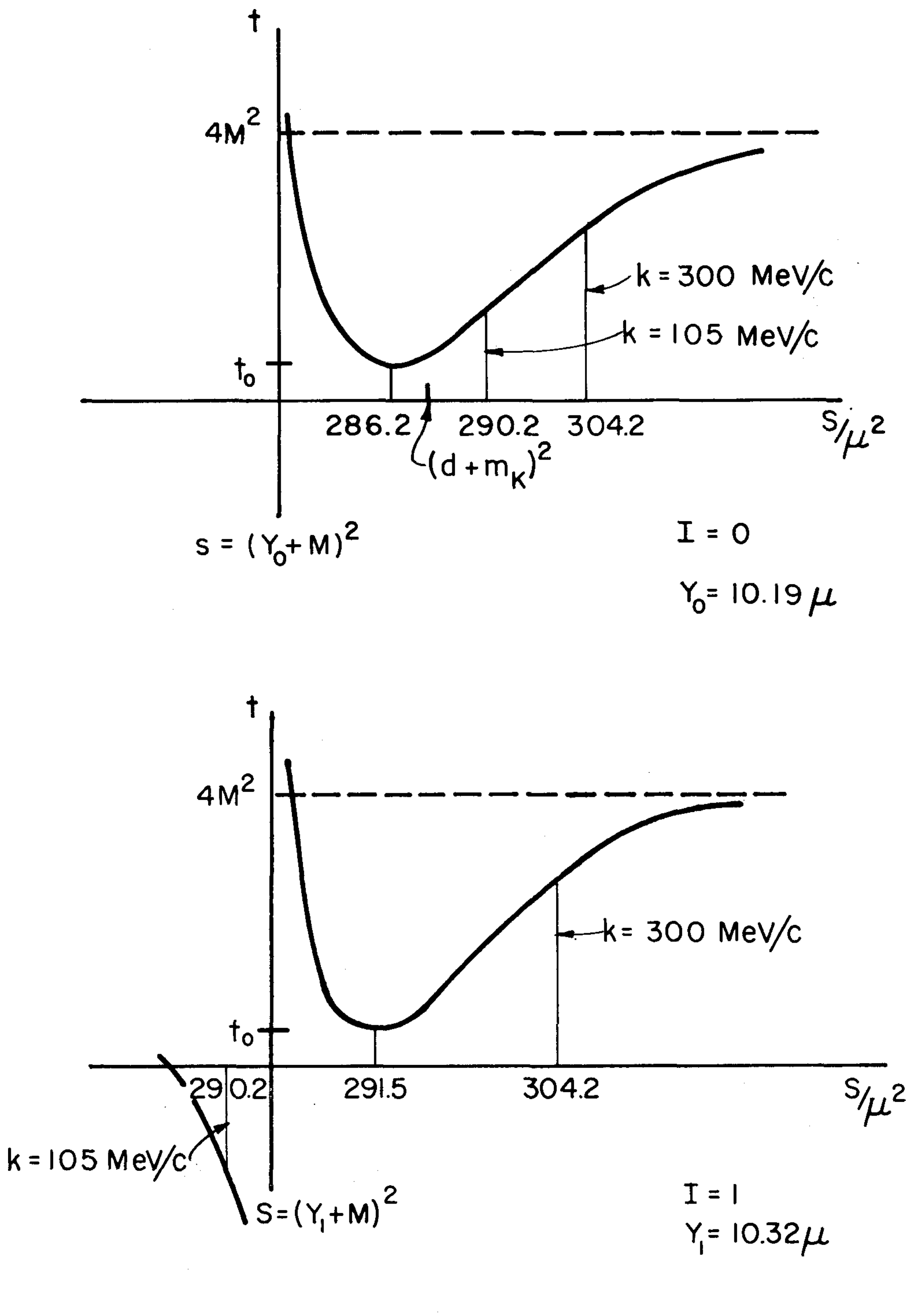
t
4M2
k = 300 MeV/c
k = 105 MeV/c
t0
286.2
290.2
304.2
S/μ2
(d + mK)2
s = (Y0 + M)2
I = 0
Y0 = 10.19 μ
t
4M2
k = 300 MeV/c
t0
290.2
291.5
304.2
S/μ2
k = 105 MeV/c
S = (Y1 + M)2
I = 1
Y1 = 10.32 μ

Fig. 20

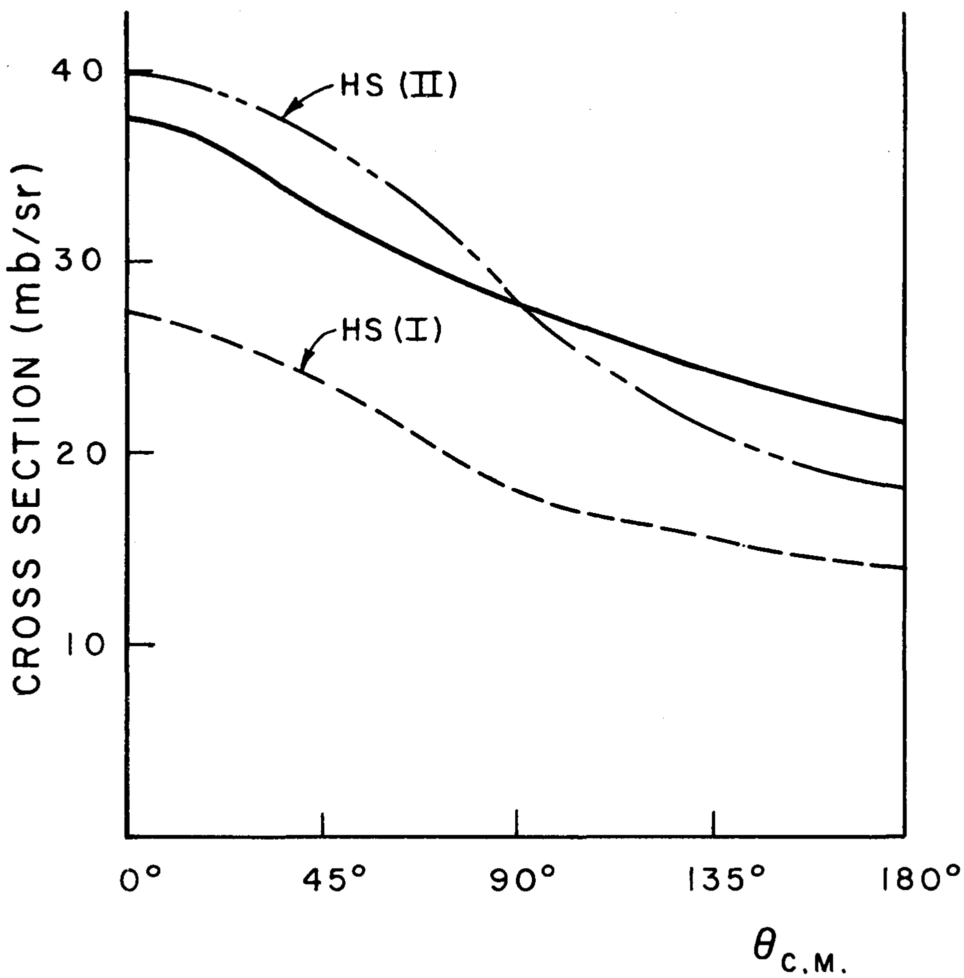

Fig. 21

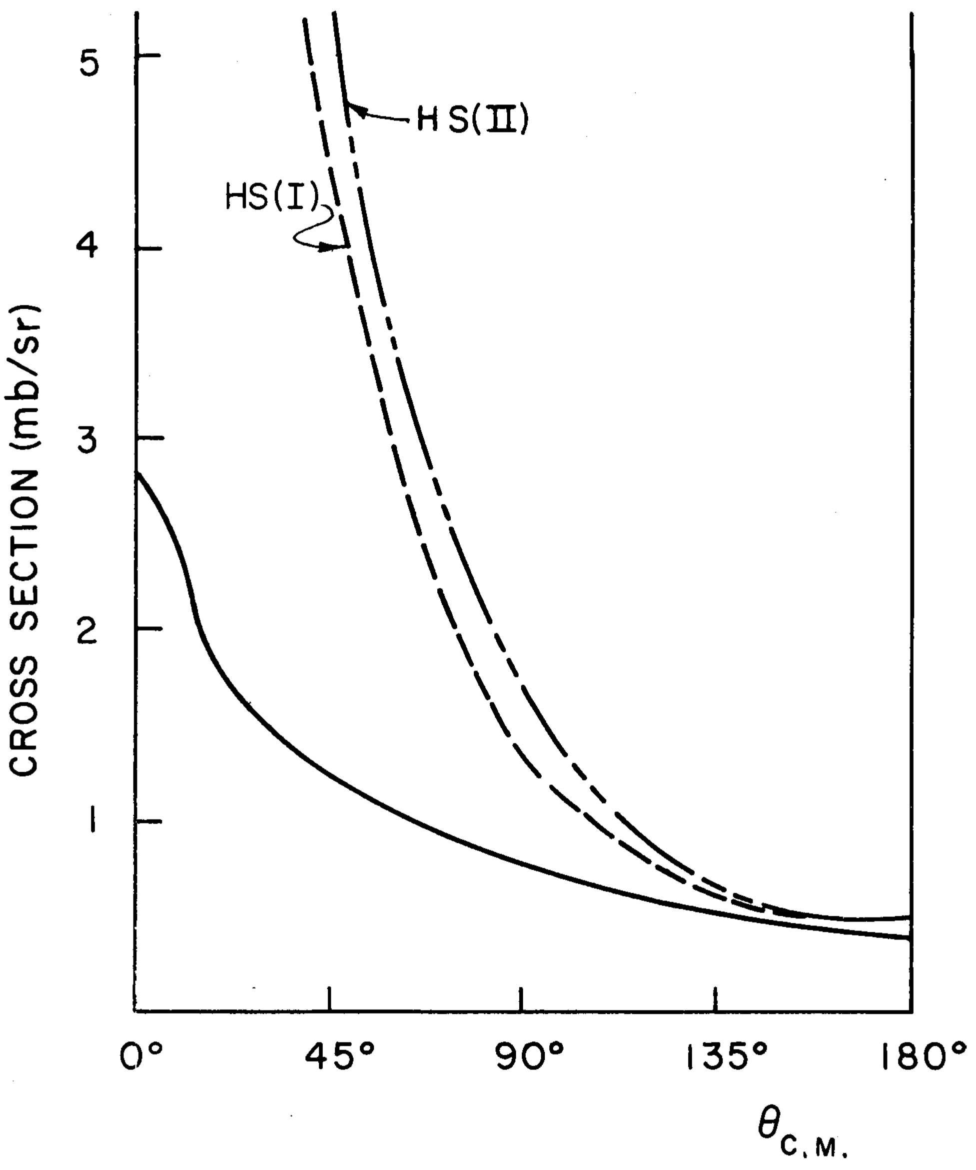

Fig. 22